Revised version, 27 August, 2020

Dear Editor,

We would like to express our sincere appreciation to the reviewers and the Editor for their interest and deep analysis of our manuscript, entitled “A new Lagrangian based short term prediction methodology for HF radar currents”. We would also like to thank the comments and suggestions they have proposed. The paper has been revised and carefully modified following those suggestions. They have undoubtedly helped to improve the quality of this manuscript.

Our individualized response to the reviews comments can be found below (the location of the main changes in the text is also indicated). We saved, as well, a version using the WORD Track Changes feature. Please do not hesitate to contact me if you think this can be useful for the review process.

Hoping the manuscript fulfils now the quality requirements of Ocean Science Journal, I look forward to hearing from you at your earliest convenience.

Yours sincerely,

Lohitzune Solabarrieta

Response to the reviewers' comments:

Reviewer #1

Dear reviewer,

We would like to show our sincere appreciation for your interest and deep analysis of our manuscript, entitled "A new Lagrangian based short term prediction methodology for HF radar currents". We would also like to thank the comments and suggestions you have proposed, they help us realize the paper needed substantial changes to allow more clarity in the presentation of methods and results. The paper has been revised and carefully modified following your advices and comments. They have undoubtedly helped to improve the quality of this manuscript. Our individualized response to your comments can be found below (in blue color).

You can find the new manuscript and the changes that we have done over it, in the final manuscript document that we will upload to the journal (both new and "track changes versions). Line references included in this document, are referred to the "track changes" version.

The manuscript describes the application of the method of analogues to the prediction of Lagrangian trajectories computed from HFR.

Lagrangian trajectories are computed from an historical data set providing surface currents from HFR systems. The catalogue of these Lagrangian trajectories is the basis to be compared to any new data set, from a present HFR surface currents. Then the future time evolution of the analogue provides the forecast for the present case.

The best analogue is selected in 2 steps. First the difference between the centroid of the 25 trajectories (the 48-h or the end position, is not clear) of each hour of the catalogue is compared with the centroid of the target field. Only the analogues resulting in a difference lower than 10km are selected. Then a Lagrangian error (\epsilon_ANL) is defined as the sum of the mean separation distance between trajectories computed from the catalogue fields and those computed from the target field, at 4 different times (6, 12, 24, 36 hours of advection). This error is in km^2. The field having the lowest error is selected and will provide the analogue forecast.

Why do we need the first step? I suppose that if \delta_cg is bigger than 10km, then the error is high? Is it for computational issues?

This step decreases the computation time. It is short (seconds to few minutes, depending on the historical dataset) but in this way, it is even shorter. It is explained in the manuscript, in the lines 336-344.

To assess the performance of the method, an equivalent Lagrangian error is computed. I'm not sure that the definitions of the errors (\epsilon_STP and \epsilon_PRS) (line 303-304 308-309) are correct. I think that the authors compute the forecast so next 48 hours instead of last 48 hours. Otherwise, I really misunderstood completely the method, which is possible, according to my numerous questions. For example, on Figure 3, I do not understand why the blue dots are the same in a) and c) (or (b) and (d)). The end points of a) shouldn't be the start points of c)? Either (a) is a backward trajectory plot, and (c) a forward plot, or again I'm missing some fundamental explanation.

You are right. ε_{STP} and ε_{PRS} are computed for forecast trajectories to compare them with realized/true trajectories, this was an unfortunate mistake in the captions. Equations' captions have been modified in the text to clarify it and a schema of all the process has also been included in the manuscript (Figure 4) with the same purpose. It is similar to the one that as you can see below, where t is the study time ant t' is the time of the best analogue. We assume that [t : (t+48)] will behave similar to [t' : (t'+48)].

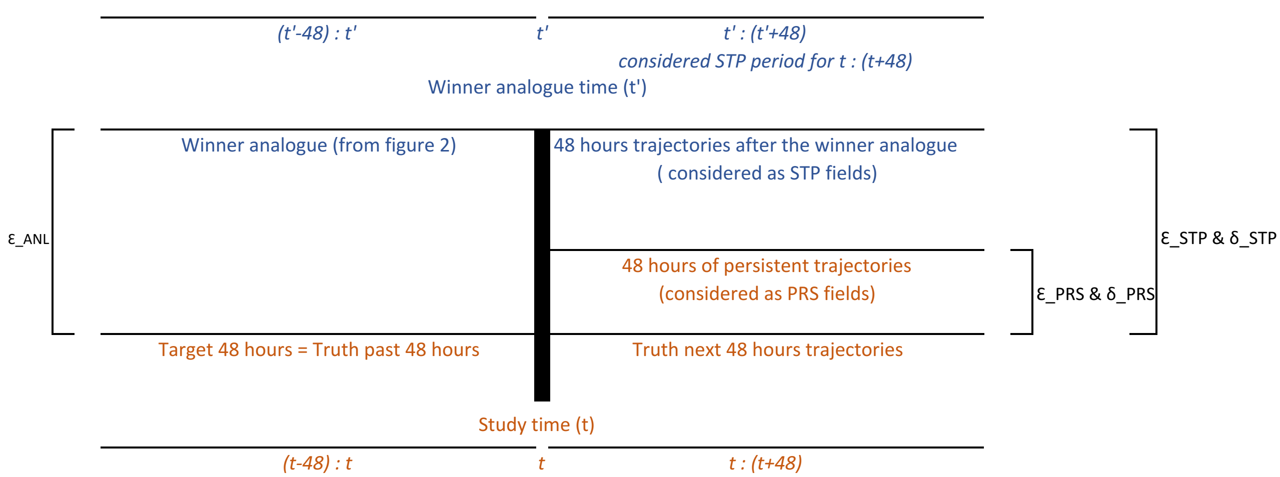

Ɛ is used to select the winner/best analogue

Ɛ_STP , Ɛ_PRS , δ_STP and δ_PRSare used to validate the methodology and estimate final error or separation distandes between real and forecast trajectories

STP fields are the forecast of the L-STP methodology

Figure 3: (now Figure 2). The blue dots are the same in all the subplots; those are the points where we initialize our simulations for 48 hours. They need to have the same starting point to be able to make comparisons between them.

So, let's assume that the authors were mistaken, and that the performance is evaluated by computing the error on the next 48 hours (forecast), by comparing the original field with the analogue forecast. Another forecast is used for comparison, based on a persistent field (constant velocity field for the future). The time series and spatial distribution of the errors have then been analyzed for 2 regions (Bay of Biscay & Black sea).

As pointed in our reply for your previous paragraph, your assumption is right and the performance is evaluated computing the error on the next 48 hours, as this will be the case in real time. And it has been analyzed for 2 regions (Bay of Biscay and Red Sea).

Figure 4 shows the time series of the errors ANL, STP and PRS. The black dots over the timeline shows the times the STP error is higher than PRS according to the caption, the other way around in the text (line 328)! At this point I was thinking to give up the reading, too many errors, to complicate to decrypt the manuscript. But let's go on. . .. PRS method seems better during winter period, since high persistent structures are present. The correlation between ANL-STP is 0.46 and ANL-PRS is 0.05. How significant are both values? Are the authors happy with the 0.46 value? Does it mean something for the methodology?

The black dots over the timeline shows the times when $\varepsilon_{STP} > \varepsilon_{PRS}$, as indicated in the caption. It has been corrected in the text (line 525-527) and it is consistent now.

Regarding the correlation values for ε_{ANL} - ε_{STP} and for ε_{ANL} - $\varepsilon_{PRS,}$ as we are comparing the errors of the past with the errors in the future (from the L-STP), we agree that the 0.46 value is low but significant. We point these values in the description of figure 4 (now converted to figure 5) in the manuscript, just to show that although during persistent periods ε_{STP} is higher that $\varepsilon_{PRS,}$ ε_{PRS} it is not correlated at all with the ε_{ANL} , while ε_{STP} shows bigger correlation, as expected.

Then the analysis is done by plotting errors (STP, PRS) or separation distances versus error_ANL comparisons are shown and discussed. Here my question is how reliable are the results in terms of the dynamics. The error values are enormous, hundreds of km^2, considering the domain size (~1.5°*1.5° according to Fig1), and the correlation coefficients quite low (maximum of 0.56 according to Table 2). Maybe a visual and qualitative comparison between the eulerian fields (the winner analogue, its forecast vs the target fields) could give an idea of the performance of the method. The values alone are not enough in my sense to validate the methodology.

As explained in our previous paragraph, the fact that the maximum correlation values between past ε_{ANL} and future ε_{STP} or ε_{PRS} is 0.56 does not mean that methodology is not working; this comparison has been done to check the goodness of our forecast compared with the past ε_{ANL} values, and to give an advice to the final user to use Persistence or L-STP as forecast.

Figures 8 and 9 (former 7 and 8) have been generated to assess the performance of the methodology. Those separation distances are similar or even better to previously published and validated results.

Maybe this method is worthwhile to be further investigated, but I would recommend to go through a major review, making the method clearer, making a methodological analysis in parallel to a physical explanation. The methodology should also be more detailed. Results should be better presented to be convincing. The analogue method was developed mainly for meteorological dynamics, which have very different time and spatial scales. Moreover, the application of this method to Lagrangian motion which very often exhibits chaotic behavior, even in regular and simple Eulerian flows, is questionable. A sub region may have analogues in one period, and a distant region another period. The authors may consider to work on sub region, and with a higher number of trajectories.

Following your advice, we have corrected the definition of the errors that we had in the first submitted version of the manuscript. We have also added a figure to make a more detailed and clearer description of the methodology.

As it is indicated in the lines 282-284 of the "track changes" manuscript, the analogues methodology was firstly applied to the Eulerian velocity fields but results were clearly worse. We later applied the method to Lagrangian trajectories as they are direct measurements of transport of substances at sea. The obtained results are similar to previously developed STP works based on HFR data (table 1) so the methodology is working fine. The main advantage of it, it is that it is simple, easily applicable in real time with previously existing codes and we can add the trajectories catalogue as we get new currents. This aspect is now better detailed in the manuscript.

The number of trajectories was widely discussed by the coauthors during the tests of the methodology. A higher number of trajectories increased computational time while the improvement of the methodology was not appreciable.

Finally, your doubt about the sub regions was also discussed by the coauthors during the tests. We tried to decompose analogue finding, not only for different periods, but also for different regions. But we discarded this option, as one of the main goals of the methodology is to give a real time and simple forecast, with low computational cost but good results. As we were interested on this and you have also suggested it, we have included this point as a future work, as it is really interesting.

Specific comments:

- Once the Error is defined (eq.1) no need to repeat it (eq.2 & 3), since the difference between the errors is not the equation, but the field used to compute the trajectories and the separation distance.

The three errors are different:

$\mathcal{E}$ (equation 1): it is the error of the target 48 hours field and each 48 hour fields of the catalogue. There is no forecast or prediction here. [min $\mathcal{E}$ =$\mathcal{E}_{ANL}$]

$Ɛ\_{STP}$ (equation 2): it is the error between the real 48 hours after the target 48hours, and the next 48 hours of the winner analogue (min Ɛ ($=Ɛ_{ANL}$) from equation 1) [which is considered as our STP forecast].

$Ɛ\_{PRS}$ (equation 3): it is the error between the real 48 hours after the target 48hours, and the 48 hours trajectory fields using the study hour as persistent currents [which is considered as our PRS fields].

As explained in previous paragraphs in this document and following your indications, the definitions have been improved in the text and a new figure (figure 4) has been also included to make the methodology clear.

- Not sure either that the definition of the time interval in line 293 is correct. Maybe the authors wanted to write v(ti)=v(tf), ti=[tf tf+48] ?

The equation is correct but it has been completed in the text to make it clearer (lines 412-413)

- Please find better definitions, and schematize the method. Instead of realized you may use truth, as for the twin experiments in data assimilation?

The definitions have been improved and the method has been schematized in the new figure 4.

"Realized" has been swapped by "truth" through the whole manuscript.

- The authors say that the method has been applied to the eulerian field with unsatis fying results (no improvement compared to other methods). Can the authors suggest some explanations for this?

Hourly HF Radar surface current fields for both study areas have more than 1000 nodes in their respective footprint areas. And each of those nodes have longitudinal and latitudinal velocity values. Moreover, the variability associated to those hourly fields is really high and we usually have to filter the data to make long time analysis of the surface currents.

In the other hand, Lagrangian trajectories measure the transport of the substances and our final goal is to minimize the separation distances between the truth and simulated trajectories. This fact, together with a lower variability associated to the Lagrangian fields, could be the reason of the better behavior of the analogue methodology with the Lagrangian fields.

- How the trajectories are computed is not explained, since the readers may not know the CODAR package. Are they purely advected? Is there any diffusion term?

In the Matlab package used in this paper, particles are advected using the HF radar hourly fields and there is no any diffusion term.

It has been included in the text (line 332)

- What is the physical significance of the error (thousand of kilometers)? - What is the distance between initial points?

The physical significance is the sum of the mean square separation kilometers at 6, 12, 24, 36 and 48 hours. It gives and approximation on how big the separation distance is between the truth and simulated trajectories.

The distance between the initial points is different for both systems:

δ_Lat=0.225 and δ_Lon=0.35 for the BoB

δ_Lat=0.1 and δ_Lon 0.15 for the Red Sea

The initial points and the trajectories to be distributed all around the study area is more important than the separation distance of the initial particles.

Reviewer #2

Dear reviewer,

We would like to show our sincere appreciation for your interest and deep analysis of our manuscript, entitled "A new Lagrangian based short term prediction methodology for HF radar currents". We would also like to thank the comments and suggestions you have proposed. The paper has been revised and carefully modified following them. They have undoubtedly helped to improve the quality of this manuscript. Our individualized response to your comments can be found below (in blue color).

You can find the new manuscript and the changes that we have done over it, in the final manuscript document that we will upload to the journal (both new and "track changes versions). Line references included in this document, are referred to the "track changes" version.

In the paper by Solabarrieta et al. a new short-term prediction method for surface marine transport is presented. The method is based on Lagrangian "analogues" calculated using velocity data from high-frequency coastal radars located in two different regions: the Bay of Biscay and the Red Sea. New-method errors and predictions are compared with those based on persistence. The performance is comparable to other methods reported in previous literature (e.g. Solabarrieta et al, 2016) as mean separation distances are shown to be similar. The new method can be more easily implemented operationally than the others due to its computational cost, which is allegedly low.

A process of major revisions is suggested to address the following concerns:

1) L123: "well demonstrated results". Please explain why OMA was chosen and quantify the OMA skills providing values and the advantages to other methodologies like DINEOF or SOM.

This paper is focused on the forecast of the surface currents and not on the gap filling techniques. This is why no more quantification values were included in the text. But we have now modified the text, to indicate that one of the main reasons to use OMAs is that it's well-functioning is demonstrated (Kaplan and Lekien, 2007, Hernández-Carrasco et al., 2018) but also because there are available codes in the HFR_progs package, that allow us not only to generate real time gap-filled fields but also to generate trajectories for our analysis (lines 148-149).

2) L138-146: not clear paragraph here and the concept may be missed. Are the authors trying to justify the choice of a Lagrangian vs Eulerian approach for the analogues? If so, wouldn't be enough to say that Lagrangian trajectories are direct measurements of transport of substances at sea? And also that they are more dependent on resolution as they are more keen on accumulating errors being integrals of the velocity fields?

We agree in this regard with referee. Accordingly, this paragraph has been rewritten in the manuscript (lines 185-187) as follows:

Lagrangian computations have proven to be robust in identifying dynamical flow structures and they are direct measurements of transport of substances at sea

3) L151: uniqueness and originality of the work. Authors should clearly state whether or not this is the first application of the method of analogues in the ocean.

It has been clarified in the text that apart from the two-fold approach of the presented method, analogue finding to generate Short Term forecast has still not been applied to HF Radar ocean surface velocity fields (lines 200-201)

4) L156: numbers expressing a quantification of the computational costs for the different methods should be provided here. How long does it take to run this new method wrt the one in Solabarrieta et al (2016)? What about wrt other methods?

As it has been included in the text, this forecast can be done in seconds or few minutes (depending on the historical dataset size) (lines 203-204).

One of the main differences with the rest of the STP methods, is that this new method is not only fast but it can also modify (increase) the historical dataset (catalogue) with the last information as soon as new data are provided, without any requirement to re-analyze the whole catalogue. This clarification has been included later on in the text (lines 741-743)

5) L162-177: how do resolutions in the two regions compare with the Rossby radii? Are spatial resolutions of the HF radars fine enough to capture the marked seasonal variability of the mesoscale features in the whole year for both regions? Please provide number and quantify.

The Rossby first radius of deformation in the red Sea is around 30 km (Zhai and Bower, 2013) and between 20 and 50 km in the BoB (~ 3-8 km over the shelf (Charria et al., 2017)). Since the spatial resolutions of both systems are 3 and 5 km respectively they resolve adequately the mesoscale in both regions.

6) L209: a conceptual question that should be addressed. It is my understanding that the OMA method is based on finding the best combination of geometrical modes in a specific region able to maximize the fit with the observations at a specific time. In a way, isn't the combination and gap-filling technique already based on "analogues" modes? Isn't this procedure already creating analogue situations from a dynamical perspective, introducing a bias when epsilon_ANL is calculated? I guess that the other way to pose the same question is: how sensitive are results to the use of OMA? How much do they change if a simple linear interpolation technique is used instead of OMA?

As pointed by the reviewer, the OMA method finds the best combination of geometrical modes in a specific region to maximize the fitting to the radar surface velocity observations. But it is not "based" in temporal analogues as this fitting is applied independently to each specific hour field, not related to the previous and later fields. Indeed, the OMA method is applied to radial velocities and it can be applied to spatial gaps (due to range fails for example) where linear interpolation technique could not be applied.

7) L213: clearly say here that the "most similar" concept will be defined later in the paper.

Included in the text (lines 273)

8) L212-218 and L220-226: more concepts are repeated in both paragraphs. Please combine them and shorten accordingly

The text has been reorganized and double concepts have been removed (lines 271-280) to make it clearer for the reader.

9) L228-230: where is this shown? I have the impression that a section has been completely cut off from the paper. This is also related to point 23 below

It has been clarified in the text that those results were done during the analysis for this work but that those results are not shown in this paper.

We want to maintain it there, as the reader may think that the direct application of the methodology to the Eulerian fields could be a better approach but we saw that it is not.

10) L237: is conceptually correct to use the whole period as a test period and a Lagrangian catalogue at the same time for the Red Sea? How do results change if the first year is used as catalogue and the second year as test period?

In the Red Sea case, it was indicated that the data availability is from July 2017 to October 2018 (2 years). This is just 1 year and 4 months and it has been corrected in the text (Line 290 in the "track control" version).

Ideally, it would be better to use past data as a training period, like the Lagrangian catalogue used for the Bay of Biscay data (because this is the situation that we will have once this method is applied in real time). But taking in account that we know (from previously published works; not HF Radar data) that there is a clear seasonality in the Red Sea study area, and the HF Radar data availability was short, we have used the whole year as a training and test period, but we have removed the previous 2.5 days and the next 2.5 days to avoid the overlapping.

11) L244: I would suggest swapping Fig.2 and Fig.3 positions as this latter is introduced in the text before.

Figures have been swapped and the references corrected accordingly in the text.

12) L269: please remove not needed.

It has been removed and the magnitude of δ_t has been indicated in line 350

13) L326-330 and Fig.4: contradictions and big confusion here. Not easy to understand whether or not black dots show periods when epsilon_STP is either larger or smaller than epsilon_PRS.

My guess is that dots are when errors in the predictions are larger than in the persistence. Please double-check and rephrase the whole paragraph

Your guess is correct. Black dots are plotted for the periods when ε_{PRS} is lower than the ε_{STP}. It has been corrected in the text (line 526) and it is consistent now.

14) L331: what is the time-scale of the persistence of these currents during winter months?

Rubio et al. (2018, 2019) and Solabarrieta et al. (2014) show that currents during winter months show an eastward flow than can least for several weeks during winter and that these currents are higher than eastward flow present during summer season.

It has been completed in the manuscript, in the first paragraph of section 3.1.

15) L343: indicatES

Corrected in the text

16) L349-357, Fig.6 and throughout the manuscript: please use the already introduced notation for the mean separation distance like, for example, \delta^STP_6h (\delta^PRS_6h) and not STP_dist (PRS_dist).

δ_{STP} or δ_{STP} has been used for the previos STP_{dist} and PRS_{dist}.

It has been modified throughout the whole manuscript and the figures.

17) L356: not sure what "especially after 12 hours mean"? Maximum values are at 36h. Do the authors want to say that larger values are reached and remain almost constant after 24h? Please rephrase.

The idea that authors want to show with the combination of figure 6 and table 2 is that there is no correlation between ε_{ANL} (used to find the analogue in the catalogue) and PRS_{dist} (distance between real and PRS simulated trajectories); while there is higher correlation between ε_{ANL} and $STP_{dist,}$ specially after 12 hours of simulation (R2(ε_{ANL} vs STP_{dist}) increases rapidly after 12 hours, from 0.37 to 0.54) as indicated in table 2)

It has been clarified in the text (lines 564-576)

18) L357: it should be also mentioned that at t=6h PRS is always better that STP (Fig.6). However we have a problem here: at t=6h R^2 for PRS is is lower than for STP

We have mentioned in the text that PRS at 6 hours is always better than STP (line 568)

Regarding the correlation, there is no any problem. From our understanding, it means that the ε_{ANL} is correlated with the STP error (bigger $\varepsilon_{ANL\ will}$ have bigger ε_{STP} or STP_{dist}) but it is no correlated with PRS error, even when persistence is better than the STP. The point here is that during the first 6 hours, it is better to use persistency than the STP. But it is worth it to use STP for longer time forecasts (for example, to predict where a possible oil spill could move).

19) L364: isn't this choice unfair wrt persistence? Shouldn't we consider all of them for a fair comparison?

With this comparison, we want to show the capabilities of the methodology for the times when we consider that the STP will be better than the Persistence ($\varepsilon_{ANL} < 853km^{2,}$ for BoB case). When $\varepsilon_{ANL} > 853km^2$, we suggest to use persistent currents

ε_{ANL} can be considered as a real-time skill-score metric for the L-STP. In fact, this value has been investigated and presented to be able to tell to the final user if our forecast is good enough or not.

20) L371: correct, it should be indeed added that persistence during the first hours is actually slightly better

It has been included in the text (line 608)

21) L380-381: why does the mean drift follow more the persistence curve in the Red Sea case?

It is probably related to temporal size of the HF Radar data availability in the Red Sea case. Longer the dataset, better results will be obtained using the presented L-STP method.

22) L390: the advantage is not clear as this is the difference between the two, does not necessarily mean that one is better than the other. Please modify Figs.9 and 10 as suggested in point 37 below

Figures 9 and 10 have been converted to figures 10 and 11, as we have included a new figure.

This point has been replied in point 37 below.

23) L404-407: what does this mean? Only Lagrangian analogues are shown in the manuscript. Has a section been cut off from the paper? This is also related to point 9 above.

As in the point 9 above, it has been again clarified in the text that those results were done during the analysis for this work but that those results are not shown in this paper.

24) L417: contradiction with L327-328

Corrected in the text.

25) L423: "first and only the first". Not really but please quantify as it looks that for BoB is at least during the first 6h and for the Red Sea at least for the first 15h!

Corrected in the text

26) L429: not sure about this value as it was reported 853 km2 before (e.g. at L342 and L364)

It was a typo mistake and it has been corrected in the text (line 671)

27) L441: Fig.7 not Fig.4, correct?

Figure 7, new Figure 8, correct. It has been corrected in the text (line 724)

28) L447-453: these lines belong more to the introduction. They are also qualitative while differences and comparisons between methods should really be quantified.

They are qualitative but we would prefer to maintain them there, as it is a comparison between both methodologies.

29) L463-472 and in general for the whole section: discussion is poor. Why aren't HF radars able to capture currents if they are persistent? I would expect radars not to be able to resolve highly-variable small-scale structures, not persistent features! Not (0.07 vs 0.19). How is this possible? getting (or buying) the idea that something persistent cannot be seen by analogues. A better dynamical insight is needed and expected in the discussion of the results.

Since temporal resolution of HF-Radars is hourly, they capture well all scales of interest above hours. This includes persistent currents. The comparison in the discussion is made between the STP system based on radars in front of a prediction made with persistence (in an abuse of language since persistence here means that the prediction for the next hour is simply the velocity measured in the last observation).

There is a reason why persistence is better during persistent periods than STP and it is not that STP does not capture persistence. It is mainly because in both cases (BoB and the Red Sea) the persistent periods show high surface velocities and the persistent structures take place in similar longitude and latitude but not exactly the same positions. A small separation distance between real and analogue fields generate high separation distances between real and simulated trajectories. But it does not happen when the real current field is used as persistent current, as it is located exactly in the place where the persistent structure is located in the study time and it will remain there at least during the first few hours.

This paragraph has been rewritten/completed in the manuscript in order to clarify and provide more dynamical insight of the presented results.

30) Fig.1: can we have GDOP maps in the two regions? Can they help discussion? Asking for more reasons: a) obtained ranges look large compared to the radar system positions and distances between them; b) it would be important to visualize in which areas OMA operations are more to be carried out; c) it would be nice to compare/discuss GDOP maps wrt to the error distributions of the new Figs.9 and 10 (see point 37 below)

Figures 9 and 10 have been converted to figures 10 and 11, as we have included a new figure.

This point has been replied in point 37 below.

31) Fig.2: resolution is really terrible, please increase it. Line should be thicker as in Figs. 7 and 8. Why are there gaps in the blue line? Really confused by the fact that caption is reporting Nov 17 2015 instead of April 13-15, 2015 as in Fig.3.

We used different examples during the writing of the manuscript and we finally did not change the date of the caption. But it is corrected now with the correct date: April 15, 2015.

There are gaps in the blue line because the methodology doesn't calculate the errors when the δ_cg > 10 km, as indicated in the text and in the caption of this figure.

We have tried to make the line thicker but we loss the details of the times when the error is not calculated because of the δ_cg > 10 km condition, as you can see in the next figure:

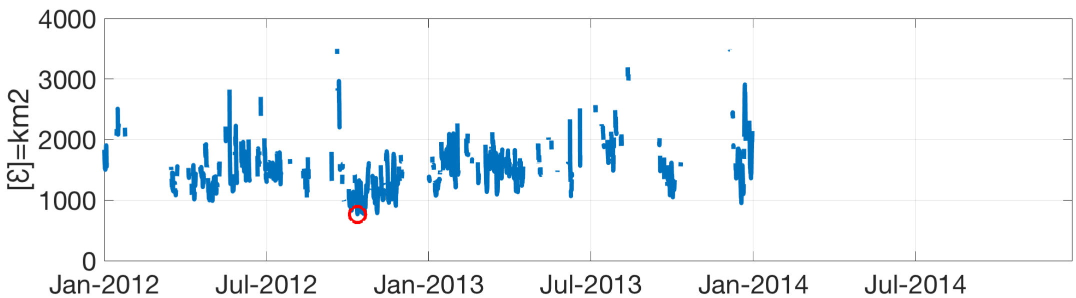

Regarding the resolution of the figure, we hope that it is just a problem with the revision version of the manuscript. We will submit a high resolution independent file to the journal for the final publication.

32) Fig.3: why is this time chosen? Is this a good or bad example?

This figure has become figure 2, following your advice.

It has been selected as an example of the good functioning of the methodology. There are better and worse examples and we wanted to show something intermediate.

33) Fig.4: resolution is really terrible, please increase it. Lines should be thicker as in Figs. 7 and 8. I would suggest to put them in three different panels as they mostly overlap. Double-check figure and text for black dots meaning.

We have modified the figure increasing the thickness of the lines. We want to maintain the three lines in just one panel to be able to see the comparison of the values. It is too complicated if we separate it into 3 panels, as you can see in the next plots:

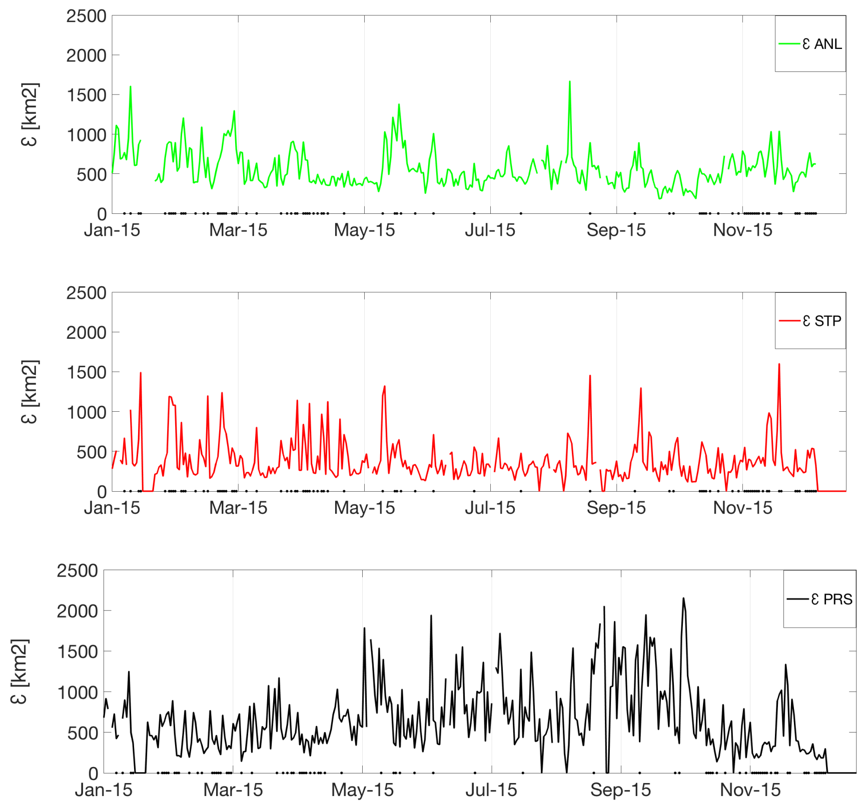

Regarding the resolution, we will proceed in the same way as with figure 2, to submit the figures with high resolution.

34) Figs.5 and 6: resolution is really terrible, please increase it. Lines should be thicker as in Figs. 7 and 8.

Modified as requested.

35) Figs.7 and 8: rearrange x-axis labels to have 6-h intervals ending at 48h.

The figure has been corrected.

36) Fig.8 caption: remove (UP)

It has been corrected in the caption.

37) Figs.9 and 10: both figures need improvements to show the errors and not only their differences. Suggestion is to have a total of 12 panels in each region and show for each time three panels, one with \delta^STP, the second with \delta^PRS and the third one with their difference.

We generated those figures before the submission of the paper and we decided to show just the difference between δ_PRS and δ_STP, as the purpose of this figures is to show the advantage (when exists) of the L-STP methodology vs the usage of persistent fields. But it may help to the reader to have them, so we could include the δ_PRS and δ_STP panels for each study area, as you suggest, as supplementary material for the paper.

As an example, we show here the results of the Bay of Biscay System:

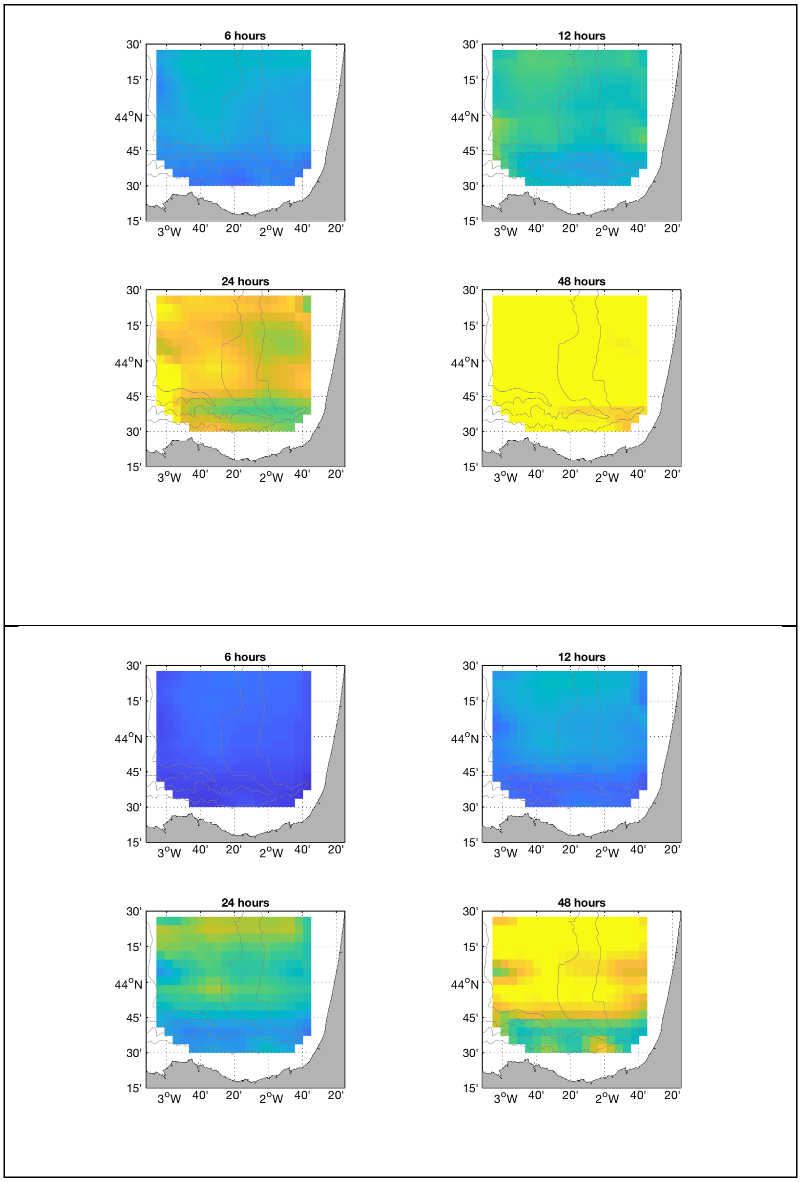

38) Figs.9 and 10: put labels indicating times either on top of each panel or in the right bottom corners, on land

Times have been included on top of each panel.

REFERENCES:

Charria G., Theetten S., Vandermeirsch F., Yelekçi Ö., and Audiffren N. Interannual evolution of (sub)mesoscale dynamics in the Bay of Biscay. Ocean Sci., 13, 777–797, https://doi.org/10.5194/os-13-777-2017, 2017

Hernández-Carrasco, I., Solabarrieta, L., Rubio, A., Esnaola, G., Reyes, E., and Orfila, A.: Impact of HF radar current gap-filling methodologies on the Lagrangian assessment of coastal dynamics, Ocean Sci., 14, 827-847, https://doi.org/10.5194/os-14-827-2018, 2018.

Rubio A., Caballero A., Orfila A., Hernández-Carrasco I., Ferrer L., González M., Solabarrieta L., Mader J. Eddy-induced cross-shelf export of high Chl-a coastal waters in the SE Bay of Biscay. Remote Sensing of Environment 205, pp. 290–304, 2018.

Rubio, A., Manso-Narvarte, I., Caballero, A., Corgnati, L., Mantovani, C., Reyes, E., Griffa, A., and Mader, J.: The seasonal intensification of the slope Iberian Poleward Current, in: Copernicus Marine Service Ocean State Report, J. Oper. Oceanogr., Issue 3, 13-18, doi: 10.1080/1755876X.2019.1633075, 2019.

Solabarrieta, L., Rubio, A., Castanedo, S., Medina, R., Charria, G., Hernández, C.: Surface water circulation patterns in the southeastern Bay of Biscay: new evidences from HF radar data. Cont Shelf Res 74:60–76 doi:10.1016/j.csr.2013.11.022, 2014.

Zhai P. and Bower A. The response of the Red Sea to a strong wind jet near the Tokar Gap in summer. Journal of Geophysical Research: Oceans, Vol. 118, 422–434 https://doi.org/10.1029/2012JC008444

A NEW LAGRANGIAN BASED SHORT TERM PREDICTION METHODOLOGY FOR HF RADAR CURRENTS

Lohitzune Solabarrieta[1,2], Ismael Hernandez-Carrasco[3], Anna Rubio[2], Alejandro Orfila[3], Michael Campbell[1], Ganix Esnaola[4,5], Julien Mader[2], Burton H. Jones[1].

(1) KAUST, Red Sea Research Center, Integrated Ocean Processes, Saudi Arabia.

(2) AZTI Marine Research, Basque Research and Technology Alliance (BRTA), Pasaia, Spain

(3) Instituto Mediterráneo de Estudios Avanzados. IMEDEA (CSIC-UIB), 07190 Esporles, Spain.

(4) Nuclear Engineering and Fluid Mechanics Dept., Gipuzkoako Ingeniaritza Eskola, Europa Plaza 1, 20018-Donostia, Spain.

(5) Joint Research Unit BEGIK, Instituto Español de Oceanografía (IEO)-Universidad del País Vasco/Euskal Herriko Unibertsitatea (UPV/EHU), Plentziako Itsas Estazioa, Areatza Pasealekua, 48620-Plentzia, Spain

Corresponding author's email: lsolabarrieta@azti.es

Deleted: LAGRANDIAN

Deleted: 4

Deleted: 5,6

Deleted: 4

Formatted: English (UK)

Deleted: AZTI Marine Research, Pasaia, Spain

Deleted: Mondragon Unibertsitatea, Faculty of Engineering, Electronics and Computer Science department, Loramendi 4, Mondragon 20500 Gipuzkoa, Spain

Formatted: Spanish

Deleted: (4) AZTI Marine Research, Pasaia, Spain

Deleted: 5

Formatted: Spanish

Deleted: 6

Formatted: Line spacing: double

Deleted: lohitzune.solabarrieta@kaust.edu.sa

ABSTRACT

The use of High Frequency Radar (HFR) data is increasing worldwide for different applications in the field of operational oceanography and data assimilation, as it provides real-time coastal surface currents at high temporal and spatial resolution. In this work, a Lagrangian based empirical real-time, Short-Term Prediction (L-STP) system is presented in order to provide short term forecasts of up to 48 hours of ocean currents from HFR data. The method is based on the finding of historical analogues of Lagrangian trajectories obtained from HFR surface currents. Then, assuming that the present state will follow the same temporal evolution as the historical analogue did, we can obtain a short-term prediction of the surface currents. The method is applied to two HFR systems covering two areas with different dynamical characteristics: the southeast Bay of Biscay and the central Red Sea. The L-STP improves on previous prediction systems implemented for the SE Bay of Biscay and provides good results for the Red Sea study area. A comparison of the L-STP methodology with predictions based on persistence and reference fields has been performed in order to quantify the error introduced by this approach. Furthermore, a temporal sensitivity analysis has been addressed to determine the limit of applicability of the methodology regarding the temporal horizon of Lagrangian prediction. A real-time skill-score has been developed using the results of this analysis which allows to identify periods when the short-term prediction performance is more likely to be low and persistence can be used as a better predictor for the future currents.

Deleted: gridded

Deleted: did

Deleted: Lagrangian

1. INTRODUCTION

The coastal zone is under increasing human pressure. On the one hand, during recent decades coastal seas have been experiencing intensified activity for recreation, transport, fisheries and marine-related energy production. Simultaneously, continued growth of the global coastal population largely contributes to increase the problem of the wastewater discharge which, in many cases, results in serious damage to coastal marine ecosystems. A better understanding of the dynamical processes responsible for the surface oceanic transport, is a prerequisite for the efficient management of the coastal ocean. These processes are responsible of the transport and fate of pollutants, nutrients, jellyfish, harmful algal blooms, plastics, etc, and improving the capacity of monitoring and forecasting the coastal area, is necessary to identify regions of accumulation or dispersion of these harmful materials. This requirement is driving the set-up of a growing number of multi-platform operational observatories designed for the continuous monitoring of the coastal ocean (e.g., US IOOS, EU EOOS, SOCIB, Australian IMOS, etc.). In the need of providing a long-term framework for the development and improvement of the European Marine coastal observations, the JERICO Research infrastrcuture has been putting efforts (through JERICO, JERICO-NEXT and JERICO-S3 projects) to develop methods and tools for the production of high-quality marine data, and the sharing of expertise and infrastructures between the exiting observatories in Europe. Moreover, due to the need of forecasting applications for response to emergency situations such oil spills, or search and rescue operations, many of the existing operational observatories are linked with operational ocean forecasting models with or without data assimilation (e.g. MARACOOS, NOAA Global Real-Time Ocean Forecast System, COPERNICUS Marine Environment Monitoring System). Typically, constituted with different in-situ point-wise observational platforms (such as moored

Deleted: experiencing increased

Deleted: increased

Deleted: Thus,

Deleted: to understand and manage these regions, and to evaluate water quality and control

Deleted: occurring near the shoreline and close offshore

Deleted: the demand for real time, operational monitoring of the coastal ocean has exploded

Deleted: a better knowledge

Deleted: of these processes

Deleted: observing systems

Deleted: -NEXT project

buoys, tidal gauges, wave buoys, etc.) a significant number of these observatories now employ land-based High Frequency Radars (HFR), that provide real-time coastal currents with unprecedented coverage and resolution (e.g. Paduan and Rosenfeld, 1996; Kohut and Glenn, 2003; Abascal et al., 2009; Solabarrieta et al., 2014, Rubio et al. 2017; Paduan and Washburn, 2013). Each HFR coastal site measures radial surface currents moving away or approaching its antenna, based in the shift of the first peak (Bragg peak) of the Doppler spectra (Crombie 1955, Barrick et al 1977). Combining the overlapping radial vectors from at least 2 antennas provides surface true vector currents (Barrick et al., 1977, Lipa and Barrick, 1983). Several studies have compared in-situ current measurements with HFR observations (e.g., Schott et al. 1985; Hammond et al. 1987; Paduan and Rosenfeld 1996, Emery et al. 2004; Paduan et al., 2006; Ohlmann et al. 2007; Liu et al., 2014; Solabarrieta et al, 2014, Bellomo et al., 2015; Lana et al., 2016; Hernandez-Carrasco et al., 2018b) and have repeatedly demonstrated the validity of this technology. Presently, more than 250 HFR antennas are installed being active worldwide (Roarty et al., 2019; http://global-hfradar.org/).

Deleted: land-based

The range and the spatial resolution of the HFR current systems depend on their working frequency and the conductivity of the water over which the system is measuring. Ranges vary from 15 to 220 km range and spatial resolution from 250 m to 12 km. Typically, a 12 MHz radar has a range ~70 km with a spatial resolution of 2-5 km. HFR systems usually average current measurements for one hour, although some average currents for shorter periods, such as 30 minutes. Due to their high spatio-temporal resolution, HFR data are commonly used in real time for search and rescue (Ullman et al., 2006) or oil spill prediction/mitigation emergency response (Abascal et al., 2017).

Deleted:

The performance of HFR for measuring near-real time surface currents has resulted in the development of assimilation strategies that incorporate the HFR measured surface currents into ocean coastal models (Breivik and Saetra, 2001, Oke et al 2002, Paduan and Shulman 2004, Stanev et al., 2011, Barth et al., 2011) some of which have been tested for short periods of time (Chao et al., 2009). However, assimilation of HFR data into models is still a computationally expensive and complex issue, not to mention operational applications of such a procedure. Because of these constrains, the availability of real-time high-resolution HFR current fields has led to alternative solutions in order to obtain short term prediction (STP) of surface coastal currents, through the direct use of HFR historical and nowcast observations using different approaches (e.g. Zelenke 2005, Frolov et al. 2011, Barrick et al., 2012, Orfila et al. 2015, Solabarrieta et al. 2016, Vilibić et al, 2016, Ren et al., 2019, see Table 1).

The above-mentioned studies develop and implement different STP approaches (harmonic analysis of the last hours, genetic algorithms, numerical models, …) which often require additional data, or long training periods of data without gaps which can jeopardize the general utility of these methods in real time (Hardware failures due to power issues, communications or environmental conditions often result in spatio-temporal gaps within HFR datasets. Spatial gaps can be filled on a real-time basis but the filling of long temporal gaps is not straightforward). Several gap-filling methodologies have been developed for HFR data sets: Open Modal Analysis, (OMA) (Kaplan and Lekien, 2007), Data Interpolating EOFs (DINEOF) (Hernandez-Carrasco et al., 2018), and Self-Organizing Maps (SOM) (Hernandez-Carrasco et al., 2018). The OMA method has been used for spatial gap filling in this paper mainly because it's well functioning has been demonstrated (Kaplan and Lekien, 2007, Hernández-Carrasco et al., 2018) and it is easily appliable in real time,

Deleted:

Deleted:). The main characteristics of these STP approaches are summarized in

Formatted: Font:14 pt

Deleted: Table 1

Formatted: Font:14 pt, Not Italic

Deleted: develope

Deleted: .

Deleted: ... [1]

Deleted: ed

Deleted: on

Deleted: data

with available codes that will also be applied for trajectories' generation, later in this paper (HFR_progs MATLAB package: https://github.com/rowg/hfrprogs).

A widely used method in time series prediction, especially in early weather forecasting, is the method of analogues. It is based on the assumption that if the behavior of a system at a given time is similar to some other situation in the historical record, then the evolution in the future of state will be similar to the evolution observed in the same historical record. Simply stated, two analogue fields are two distinct fields that are close enough considering some metric, to be considered as equivalent. The finding of the best (nearest) analogue of a specific time does not require a historically continuous dataset, as long as it contains subsets of observations that extend longer than the testing period. These analogue events occur naturally in the environment and this methodology has been applied and tested in atmospheric forecasts (Lorenz, 1969, Jianping et al,1993, Prince and Goswami 2007, Shao and Li 2013).

Given the motivation described above, and developed partially in the framework of JERICO-NEXT project, we present a Lagrangian-based Short-Term Prediction (L-STP from now on) methodology using existing HFR datasets, to be applied to current real-time observations. The uniqueness of this approach is two-fold: first the historical Eulerian velocity fields are used to construct a catalogue of Lagrangian trajectories and second, using the trajectories obtained from present observations, analogues in the past dataset are searched in order to obtain the best predictive match. The method is based on Lagrangian computations since they have proven to be robust in identifying dynamical flow structures and they are direct measurements of transport of substances at sea.

Deleted: and it has well demonstrated results (Kaplan and Lekien, 2007).

Formatted: Font:14 pt

Deleted:

Deleted:

Formatted: Font:Times New Roman, 14 pt, Font color: Auto

Formatted: Font:Times New Roman, 14 pt, Font color: Auto

Formatted: Font:Times New Roman, 14 pt, Font color: Auto

Formatted: Font:Times New Roman, 14 pt, Font color: Auto

Formatted: Font:Times New Roman, 14 pt, Font color: Auto

Formatted: Font:Times New Roman, Font color: Auto

Deleted: simple

Moved (insertion) [1]

Deleted: Lagrangian diagnostic will capture dynamical features present in the flow that are not readily apparent in pure velocity. At this point we remark that they are more dependent on resolution since they are more keen on accumulating errors being integrals of the velocity fields

Then, it is worth highlighting that this is the first time that the analogues technique is applied to the HFR-derived ocean surface currents to obtain short-term forecast. The L-STP is intended to be implemented operationally requiring low computational cost (seconds to few minutes for each forecast, depending on the size of the historical dataset) and it is easy to implement using existing HFR data processing tools.

Deleted: Moreover

Deleted: has still not been

Deleted: HF Radar velocity field’s

Deleted: is new real-time Lagrangian based short-term prediction methodology

2. *DATA AND METHODS*

2.1 Data

HFR data from two distinct oceanographic regions have been used for the evaluation, validation and testing of the developed methodology in this paper (Figure 1): Left: The Bay of Biscay (hereinafter BoB HFR) and Right: The central Red Sea region (hereinafter Red Sea HFR). These two study regions are used to evaluate the skill of the method with different dynamical conditions, and with a sufficient set of observations to provide a database suited to the efficient research of appropriate analogues. The BoB HFR system, located in the southeastern corner of the Bay of Biscay, in the Basque Country, is composed of two CODAR Seasonde sites, working since 2009 which transmit at 4.5MHz frequency covering up to 200km range and providing hourly surface velocity field at 5 km of spatial resolution. The dataset used in this study spans the period from 2012 to 2015. The Red Sea HFR system is located on the central western coast of Saudi Arabia and is also composed of two CODAR Seasonde sites, operational since June 2017, transmitting at 16.12MHz frequency, covering up to 120 km range and providing the hourly surface velocity field at 3 km spatial resolution. The dataset from June 2017 to October 2018 has been used in this study.

The BoB HFR has been chosen as the pilot system for testing the developed methodology because of our previous knowledge regarding the circulation and dynamical processes in the study area (Rubio et al 2013, Solabarrieta et al 2014, Solabarrieta et al., 2015, Rubio et al., 2018, Hernandez-Carrasco et al. 2018). The resulting methodology is then applied to the operational Red Sea HFR dataset, as a study case. Coastal dynamics in the BoB show a clear seasonality where cyclonic and anticyclonic eddies dominate in winter and summer, respectively in responding

Formatted: Font:Not Italic

Formatted: Check spelling and grammar

Deleted: Figure 1

Deleted: from which to find

to local winds and the mean coastal current (Iberian Poleward Current) (Esnaola et al., 2013, Solabarrieta et al., 2014). The circulation in the the central Red Sea also demonstrates a clear seasonality (Sofianos and Johns, 2003; Yao et al., 2014a, 2014b; Zarokanellos et al., 2016, 2017) linked to the seasonal winds of the area (Abualnaja et al., 2014; Langodan et al., 2017). The region is dominated by eddy activity, with both cyclonic and anticyclonic eddies dominating the region (Zhan et al., 2014; Zarokanellos et al. 2016). Due to the only recently available dataset (since mid-June 2017 to present) the detailed small-scale surface circulation processes of this area is under characterization at the moment.

Deleted: area covered by

Deleted: HFR

The primary difference between the two HFR systems is the operating frequency (5MHz for the BoB system and 16 MHz for the Red Sea system) resulting in a larger spatial coverage for the BoB HFR than for the Red Sea HFR (200km range vs. 120km, respectively), but with higher spatial resolution for the latter (3km and 5 km, respectively). This difference in the spatial resolution should result in better capturing the small-scale dynamical features in the Red Sea that could influence the selection of an analogue.

Deleted: Red Sea HFR than for BoB HFR

Deleted: in

The data from both systems have been processed similarly. The spectra of the received backscattered signal are converted into radial velocities using the MUltiple SIgnal Classification (MUSIC) algorithm (Schmidt 1986). HFR Progs MATLAB package is then used to combine radial currents and generate gap-filled total 2D currents, using the Open Modal Analysis (OMA) methodology of Kaplan and Lekien (2007).

Deleted: (https://cencalarchive.org/~cocmpmb/COCMPwiki)

2.2 Lagrangian analogues

The proposed methodology is based on the analogue finding approach, using a historical catalogue of maps of Lagrangian trajectories and finding the most similar one (detailed later in this section) to that of the last 48 hours (target field). Then, the next 48-hour time evolution of the closest (chosen) analogue provides the forecast for the target period. In other words, if we find a state in the historical database that is close enough to the target field (given a metric), the forecast for the current observations will evolve in the same way as did for the chosen analogue. Analogue finding has been applied in several geophysical variables in different regions (Zorita and von Storch, 1999; Fernandez-Ferrero et al., 2009, 2010; Ibarra-Berastegi et al., 2011; Martin et al., 2014; Seubert et al., 2014; Ibarra-Berastegi et al., 2015).

The analogue finding was first applied to eulerian surface velocity fields of the BoB HFR System (not shown), but the results did not improve the previously published STP results for the study area. The methodology was tested subsequently using a four-year dataset (2012-2015) of trajectory maps computed for the SE BoB, where the trajectory maps from the three first years was used as the search catalogue for analogues (2012-2014) (hereinafter "Lagrangian catalogue"), and the remaining year (2015) was used as a test case (hereinafter "test period"). Then the method was applied to the Red Sea dataset, for the period of July 2017-October 2018. As the period was short (1 year and 4 months), we have used the whole period to build the Lagrangian catalogue and act as a test period at the same time. In this case, for the analogues search the 5-days period around the date of the target field was removed from the catalogue at each iteration, to avoid temporal overlapping with the target field.

Deleted: Lagrangian
Deleted: the
Deleted: one of
Deleted: and use it as the closest, chosen analogue
Deleted: future
Deleted:
Deleted: present case
Deleted: period
Deleted: the historical chosen period
Deleted: The method embeds trajectories of particles in a state space using delay coordinates.
Deleted: ... [2]
Deleted: later
Deleted: a
Deleted: with
Deleted: BoB
Deleted: fields belonging to the
Deleted: are
Deleted: ") from where we extract the last 48-hour's target field trajectories (hereinafter "target field") every hour (excluding the last/previous 48 hours)
Deleted: has been
Deleted: is
Deleted: 2
Deleted: s
Deleted: and Lagrangian catalogue
Deleted: e
Deleted: e
Deleted: the
Deleted: For the catalogue period,
Deleted:
Deleted: 2.5 previous and 2.5 next days from
Deleted: are

To build the Lagrangian catalogue we first generated hourly fields of 25 virtual particle trajectories on a regular grid, blued dots of Figure 2), which were advected by the OMA HFR surface currents (without considering diffusion) during 48 hours. To this end we used the Lagrangian module included in the HFR_Progs MATLAB package, following the same procedure for the test period. Then, for each hour of the test period, the method searched the most similar Lagrangian patterns in the Lagrangian catalogue dataset. To increase the efficiency of the processes, the search was done in two steps. First, we looked for potential analogues with a similar main drift. To do that we computed and compared the position of the centroid of the 25 trajectories of each analogue to that of the target field, and discarded the analogues whose centroid was at a distance > δ_cg. The value of the δ_cg needs to be small enough to minimize computational time but sufficiently large to as to not lose potential analogues. We explored different values of this distance threshold and we found that δ_gc=10km produces a good compromise between computational cost and number of potential analogues in both study areas. Then, in a second step, we computed the Lagrangian errors (Ɛ) between the trajectories of the target field and the potential analogues, defined as:

$$\mathcal{E} = \Sigma\left((\delta\_{6h})^2 + (\delta\_{12h})^2 + (\delta\_{24h})^2 + (\delta\_{36h})^2 + (\delta\_{48h})^2\right) \qquad \text{Eq. (1)}$$

Where δ_t is the mean separation distance [km] at time t between the trajectories belonging to the target field and each of the potential analogues (being t=6, 12, 24, 36 and 48 hours inside the trajectories lifetimes).

Finally, the potential analogue with the lowest Ɛ was selected as the best analogue ($\mathcal{E}_{ANL}$= min (Ɛ)) and the velocity fields during the next 48 h from that analogue provides STP currents for the target period (hereinafter "L-STP fields"). *Figure 3*

Deleted: dataset
Deleted: purely
Deleted: in the HFR velocity field using a regular grid of initial positions (Nº= 25, Blue dots of Figure 2Figure 3) inside the HFR gap-filled OMA current fields domain
Formatted: Font:Not Italic, Font color: R,G,B (16,16,16)
Deleted: -
Deleted: was used to compute the trajectories (previously employed to generate the OMA fields)
Deleted: . We follow the
Deleted: F
Deleted: s
Deleted: his process
Deleted: i
Deleted: particles during their 48-h
Deleted: the potential
Deleted: with respect to the position of the centroid for
Deleted: ter of gravity is
Deleted: (δ_gc=10km in both HFR systems) from the center of gravity of the final positions of the target field
Deleted: cases
Deleted: Continuing the selection of the analogue process
Deleted: fields of the Lagrangian catalogue
Formatted: Normal, No bullets or numbering
Deleted: :
Deleted: Lagrangian catalogue field
Deleted: or
Deleted: in the last 48 hours
Deleted:
Deleted: [Ɛ]=km^2 ... [3]
Deleted: Lagrangian catalogue's field
Deleted: error (
Deleted:)
Deleted: -in terms of Lagrangian distances- in comparison with the target field
Deleted: is
Deleted: the following 48 hours of
Deleted: the forecasted
Deleted: *Figure 4*

shows an example of the values of Ɛ, through the potential analogues for a specific case.

Figure 2 provides an example of the selected analogue (Figure 2b) and corresponding L-STP fields (Figure 2d) for a given target field (Figure 2a) and the 'truth' trajectories for the following 48 hours from the date of the target field (Figure 2c). The associated temporal series of errors for the target field and the potential analogues are shown in *Figure 3*, where the value of ε_{ANL} is marked using a red dot. (corresponding to the error between the trajectories of the L-STP field in Figure 2d and the truth trajectories for the forecast period in –Figure 2c).

To assess the performance of the methodology, we computed forecasted trajectories based on persistence of currents (hereinafter 'persistence fields'). To obtain simulated trajectories using persistence currents, the particles were advected during 48 hours using a constant velocity field (target field) during the 48 hours of simulation:

$$v(x,y,tf+ti)= v(x,y,tf),$$

where tf= study time and ti=[tf: tf+48h].

The mean drift of the truth forecasted trajectories is also computed for each simulation period (the means drift is considered as the average of the distances moved by each particle during 48 hours).

The Lagrangian errors between the truth trajectories and the L-STP and between the truth trajectories and the persistence field were also computed as follows:

Deleted: Figure 2

Deleted: the errors,…Ɛ, through the potential analoguesLagrangian catalogue ... [4]

Deleted: Figure 3

Deleted: Figure 3

Formatted ... [5]

Formatted ... [6]

Deleted: Figure 3

Formatted ... [8]

Deleted: Figure 3…a) and the 'realized ... [9]

Formatted ... [7]

Deleted: after

Deleted: the

Formatted ... [10]

Deleted: Figure 3

Deleted: in the Lagrangian catalogue

Deleted: …*Figure 3Figure 3Figure* 4…Figure 2 ... [11]

Deleted: minimum error for the …alue of selected analogue (…$_{ANL}$)…is marked in ... [12]

Formatted ... [13]

Deleted: Figure 3…d and the realized ... [14]

Formatted ... [15]

Deleted: Figure 3…c). ... [16]

Deleted: have …omputed forecasted trajectories based on persistence of currents (hereinafter 'persistencet…fields'). To obtain simulated trajectories using persistence currents, the velocity field of target field at t=tf are kept constant and the particles are …ere advected during 48 hours using ... [17]

Formatted: Spanish

Formatted: Indent: First line: 0.6"

Deleted:

Deleted: realized

Comment [AR3]: the centroid??

Deleted: realized

Deleted: forecast …-STP and between the truth trajectories and the persistence field/Persistent currents…werehave…also been defined and computedalculated ... [18]

$$\varepsilon_{STP} = \Sigma\left((\delta\_{6h})^2 + (\delta\_{12h})^2 + (\delta\_{24h})^2 + (\delta\_{36h})^2 + (\delta\_{48h})^2\right) \qquad \text{Eq. (2)}$$

where δ_t is the mean separation distance between truth field's and the L-STP field trajectories for t= t ; t+48 (following 48 hours from the study time)

Deleted: realized

Deleted: -48

Deleted: -1

Deleted: last

$$\varepsilon_{PRS} = \Sigma\left((\delta\_{6h})^2 + (\delta\_{12h})^2 + (\delta\_{24h})^2 + (\delta\_{36h})^2 + (\delta\_{48h})^2\right) \qquad \text{Eq. (3)}$$

where δ_t is the mean separation distance between truth field's and Persistent field trajectories for t= t : t+48 (following 48 hours from the study time)

Deleted: realized

Deleted: -48 :

Deleted: -1

Deleted: last

All the process for the selection and validation of the analogue with the different variables has been summarized in *Figure* 4.

Deleted: diferent

The time series and spatial distribution of the ε_{STP} and ε_{PRS} errors have been analyzed for both study areas. Finally, ε_{STP} and ε_{PRS} time series have also been calculated and compared to the time series of the ε_{ANL}, in order to evaluate if the ε_{ANL} can be used as an indicator of the expected skill of the L-STP with respect to the persistence.

Deleted: errors of the L-STP (

Deleted:)

Deleted: persistence fields (

Deleted:)

3. RESULTS

The performance assessment results for the BoB HFR system are described in section 3.1 and the temporal and spatial forecast for both study areas are shown in section 3.2.

3.1 Assessment of the L-STP skills

Figure 5 shows the ε_{ANL} through year 2015 for the BOB study area, together with the ε_{STP} and ε_{PRS}. The mean value of the ε_{PRS} is 73% higher than the ε_{STP}. Black dots over the timeline in Figure 5 show the times when ε_{STP} is higher than the ε_{PRS}, which occurs 12% of the time. Focusing on the times when the ε_{PRS} is lower than the ε_{STP} (black dots of the timeline in Figure 5), it can be seen that they mostly occur during winter months. Previous works in this area have shown that there are high persistent eastward currents that can least for several weeks during winter months (Solabarrieta et al., 2014), which can explain the better performance of the persistence fields in this period.

The correlation between ε_{ANL} and ε_{STP} is 0.46 while correlation between ε_{ANL} and ε_{PRS} is 0.05, for the whole test year (2015) (Figure 5).

The hourly values of ε_{STP} and ε_{PRS} have been plotted against their corresponding hourly ε_{ANL} values for the test year, ordered from minimum to maximum along the x-axis in Figure 6. We observe that, when ε_{ANL} is low (less than 853 km^2 for this data set), ε_{STP} is smaller than ε_{PRS}. However, as ε_{ANL} increases, ε_{STP} and ε_{PRS} converge until an inflection point beyond which ε_{STP} is slightly greater than ε_{PRS}. For the SE BoB experiment, the inflection point occurs at ε_{ANL} =853 km^2 and 88% of cumulative

Deleted: demonstrated

Deleted: As described in the methodology, for each hourly time step in the data, the best analogue for that time step was found (the one with ε_{ANL} =min (ε))

Deleted: .

Formatted: Font:Not Italic

Deleted: Figure 4

Deleted: ro

Formatted: Check spelling and grammar

Deleted: Figure 4

Deleted: lower

Formatted: Font:Not Italic

Deleted: 75.41

Formatted: Font:Not Italic

Formatted: Check spelling and grammar

Deleted: Figure 4

Deleted: is reflected in these results

Deleted: .

Formatted: Font:Not Italic

Formatted: Check spelling and grammar

Deleted: Figure 4

Deleted: (red)

Deleted: (blue)

Formatted: Font:Not Italic

Formatted: Check spelling and grammar

Deleted: Figure 5

Deleted: less

ε_{ANL}. Results from the Red Sea HFR system indicates a similar pattern (not shown), when the inflection point occurs at $\varepsilon_{ANL} = 821$ km^2 and at 86.4% of cumulative ε_{ANL}.

Further analysis to elucidate the time periods that largely contribute to the errors, compared to persistence are presented hereinafter. ε_{ANL} has been plotted together with the mean separation distances of the trajectories using STP and persistent currents (hereinafter δ_{STP}, δ_{PRS}), after 6, 12, 24, 36 and 48 hours for each target field (Figure 7). δ_{STP} is always higher than the δ_{PRS} for the 6 hours' simulation. But the values of δ_{STP} show better results for simulations at 12, 24, 36 and 48 hours. The values of the correlation coefficient (R^2) between the ε_{ANL} and δ_{STP} and between ε_{ANL} and δ_{PRS} after 6, 12, 24, 36 and 48 hours are summarized in Table 2. Values of R^2 for ε_{ANL} and δ_{PRS} are small (almost no correlation), varying between 0.01 and 0.11, while correlations between ε_{ANL} and δ_{STP} are higher, varying between 0.19 and 0.56, and showing higher correlation (>than 0.39) after 12 hours of simulations. The behavior of the Red Sea HFR system figures (not shown) is similar to the BoB HFR system.

3.2 L-STP performances in the selected study areas

Mean separation distances between truth and forecasted trajectories after different periods of integration times have been computed for both systems, for the best analogues, i.e., before the inflection point of $\varepsilon_{STP>}\varepsilon_{PRS}$ (Figure 6), in order to evaluate the temporal forecast capabilities of the methodology. Only analogues with $\varepsilon_{ANL} <$ 853km^2 (BoB system) have been used to generate this analysis, as those are the periods when the methodology produces good results. Separation distances computed for the whole test year 2015, are shown in Figure 8, for the BoB HFR observations.

Deleted: s

Deleted: has

Deleted: ed

Formatted: Not Highlight

Deleted: STP_{dist} and PRS_{dist}

Deleted: Figure 6

Formatted: Font:Not Italic

Formatted: Check spelling and grammar

Formatted: Subscript

Formatted: Subscript

Formatted: Subscript

Deleted: STP_{dist}

Formatted: Subscript

Deleted: PRS_{dist}

Formatted: Font:14 pt, Not Italic

Formatted: Font:14 pt

Deleted: Table 2

Formatted: Subscript

Deleted: PRS_{dist}

Formatted: Subscript

Deleted: for

Deleted: STP_{dist}

Formatted: Subscript

Deleted: especially

Deleted:

Formatted: Subscript

Deleted: realized

Deleted: functioning

Formatted: Font:Not Italic

Formatted: Check spelling and grammar

Deleted: Figure 5

Deleted:

Formatted: Font:Not Italic

Formatted: Check spelling and grammar

Deleted: Figure 7

The separation distances between the measured trajectories and predicted persistent and STP trajectories, have similar values during the first 6 hours (4km) of the forecast period, with slightly better results for persistent trajectories. But after 6 hours, the separation distance for the forecast based on persistent currents increases faster than using L-STP. At 24 hours, the separation distance is 11 km for persistence forecasts and 8km for L-STP forecasts. The values are 12 and 18km, respectively, after 48 hours of simulation. The mean drift values of the truth trajectories show that the mean drift is similar to the L-STP separation distances, during the 48 hours.

Temporal mean separation distances between truth and forecasted trajectories for the Central Red Sea HFR System, computed for the whole test time, are shown in Figure 9. Only the best analogues with ε_{ANL} less than inflection point, i.e., $\varepsilon_{ANL} < 821km^2$, have been used to generate this analysis. The separation distances for the STP forecasts are higher than those forecasts with persistent currents during the first 15 hours. After 15 hours, quality of forecasts reversed where STP produced better results than persistence.

Spatial distribution of the difference between δ_{PRS} and δ_{STP} at 6, 12, 24 and 48 hours, for the BoB and the Red Sea study areas, are shown in Figure 10 and Figure 11.

For the BoB HFR system, the differences are not appreciated during the first 6 hours. But after 12 hours of simulation, the advantage of the L-STP is clear in most of the study area, especially outside the continental shelf slope where persistent currents dominate the circulation. The separation values between δ_{PRS} and δ_{STP} increase up to 10km after 48hours of simulation.

Deleted: ‘
Deleted: realized
Deleted: ’
Deleted: realized
Deleted: (July 2017-October 2018),
Formatted: Font:Not Italic
Deleted: Figure 8
Deleted: winner
Formatted: Check spelling and grammar
Deleted: STPdist
Formatted: Subscript
Formatted: Subscript
Deleted: PRSdist
Formatted: Subscript
Deleted: HFR systems
Formatted: Font:Not Italic
Deleted: Figure 9
Formatted: Font:Not Italic
Formatted: Check spelling and grammar
Deleted: Figure 10
Formatted: Subscript
Deleted:

For the Red Sea, the significant differences between STP and Persistence start after 24 hours of simulation, and continue until 48 hours.

Deleted: HFR system

4. DISCUSSION

In this work, a new methodology to forecast HFR currents has been described and the skill of the proposed STP methodology is analyzed. Different analyses are performed in order to check the spatial and temporal capabilities of the proposed methodology.

The methodology is based on the search of analogues in a trajectory (Lagrangian) space using a previously generated trajectory field catalogue. The values of the δ_{STP}, compared to previous works in the BoB area showed that the L-STP produces accurate predictions, which demonstrates the ability of the Lagrangian approach to capture key dynamical features needed to accurately predict the proper dynamical conditions.

Significant correlation values between ε_{ANL} and δ_{STP} , suggest that the ε_{ANL} can be considered as a real-time skill-score metric for the L-STP. Both BoB and the central Red Sea show a similar behavior; although the ε_{ANL} values are different, the accumulative % of the transition point is similar in both cases.

Figure 7 shows that after 12 hours of simulation, the L-STP provides a better prediction than the persistence field for more than 80% of the cases (reaching more than 90% of the cases for 36 and 48 hours of simulation). The minimum ε_{ANL} value for the δ_{STP} and δ_{PRS} cross point is 714km^2. Figure 6, for the total ε_{ANL} shows the same behavior being 853km^2 the transition analogue error value between STP and Persistence.

Deleted: were

Deleted: The analogue finding was first applied to surface velocity fields (not shown in this paper) rather than in the trajectory space of the BoB HFR System, but the results did not improve the previously published STP results for the study area. Analogue finding method was later applied to Lagrangian trajectory fields, advected using the HFR velocity fields

Deleted: STP_{dist}

Formatted: Subscript

Deleted: analogue finding

Deleted: more

Deleted: if it is applied to Lagrangian trajectories than does the application to surface current velocities. This shows

Deleted: C

Deleted: $PRS_{dist}\delta_{PRS}$ vary between 0.01 and 0.11, showing no significant correlation (Table 2Table 2). The values using STP_{dist}

Formatted: Subscript

Formatted: Font:14 pt, Not Italic

Formatted: Font:14 pt

Formatted: Subscript

Moved (insertion) [2]

Deleted: The results

Deleted: are higher, varying between 0.19 and 0.56 (Table 2Table 2 and Figure 7Figure 6). During the test period for the BoB HFR system, ε_{STP} is lower than the ε_{PRS} about 88% of the time (Figure 6Figure 5). The 12% of the time when the persistence results are better (black dots over the time ... [19]

Formatted: Font:14 pt, Not Italic

Formatted: Font:14 pt

Formatted: Font:Not Italic

Formatted: Font:Not Italic

Formatted: Font:Not Italic

Deleted: As stated in previous work, that the circulati ... [20]

Formatted: Font:Not Italic

Deleted: Figure 6

Deleted: forecast

Deleted: prediction from P

Deleted: STP_{dist}

Formatted: Subscript

Deleted: PRS_{dist}

Deleted: Figure 5

Formatted: Subscript

Formatted: Font:Not Italic

Deleted: 15

For the BoB HFR System, temporal δ_{STP} shows values of 3.5km, 5.5km and 8km, after 6, 12, and 24 hours respectively. The δ_{STP} values are similar to the δ_{PRS} values during the first 6 hours of simulation but δ_{STP} are lower after that, with 3km and 5.5km of difference between them, after 24 and 48 hours of simulation, respectively (*Figure* 8). As stated in previous work, that the circulation over the BoB area is dominated by a stable, persistent current field during winter (Solabarrieta et al., 2014) which is reflected by these results where persistence has good or even slightly better forecasting skill during the first 6 forecast hours than the proposed methodology.

The δ_{STP} values for the BoB HFR system are similar to the ones obtained by Solabarrieta et al., 2016, for the whole year but δ_{STP} are better for summer months, for the same study area. They used the linear autoregressive model, described in Frolov et al., 2012, to forecast HFR current fields and the errors using that approach were 2.9 and 7.9km after 6 and 24 hours. Although the results obtained in this work improve only during certain periods the forecast presented in Solabarrieta et al. 2016, the presented methodology has three advantages over the previous method: it is easily run in real time; it does not require a continuous training period; and it is able to discriminate the times when the usage of the persistence is applicable. On the negative side, it requires the generation of a catalogue of past trajectories as the search space for analogues, but once it is ready, it is easily increasable in real time, without extra pre-analysis; just adding new trajectory fields to the previous catalogue.

Moved up [2]: The results suggest that the ε_{ANL} can be considered as a real-time skill-score metric for the L-STP. Both BoB and the central Red Sea show a similar behavior; although the ε_{ANL} values are different, the accumulative % of the transition point is similar in both cases.

Deleted: STP_{dist}

Formatted: Subscript

Deleted: STP_{dist}

Formatted: Subscript

Deleted: PRS_{dist}

Formatted: Subscript

Deleted: STP_{dist}

Formatted: Subscript

Deleted: Figure 4)

Deleted: STP_{dist}

Formatted: Subscript

Deleted: STP_{dist}

Formatted: Subscript

Deleted: .

The values of the δ_{STP} for the Red Sea HFR system follow a similar pattern to the BoB results, with higher separation distances. This may be related to the limited time span of the available dataset, as a better closest analogue may be found in a longer dataset.

The spatial comparison of the δ_{STP} and δ_{PRS} for the BoB HFR system (Figure 10), shows that the L-STP has better skills for the entire study area after 12 hours of simulations. The skills of the L-STP with respect to the persistence increases with time, showing up to10km of improvement relative to persistence at 48 hours in some parts of the study area. For the spatial distribution, after 12 hours, the smallest differences between δ_{STP} and δ_{PRS} occurred over the slope. This is explained by existence of persistent seasonal Iberian Poleward Current that flows along the continental slope toward the east along the Spanish coast and northward along the French coast (Solabarrieta et al. 2014). In other words: although the L-STP can be performant in periods of persistent currents, the persistence field can show a better forecast for a short temporal scale (48h), L-STP will improve those forecasts, as soon as spatiotemporal variability increases.

The results for the Red Sea HFR system are similar but the benefit of the L-STP methodology appears only after 12 hours of simulation. Spatially, the improvement is again lower where persistent currents occur, as it is the case of the Eastern Boundary Current that flows northward following the eastern Red Sea Coastline in the study area (Bower and Farrah, 2015; Sofianos and Johns, 2003; Zarokanellos et al., 2017). The dominance of the persistent currents is evident in the lower values of the difference between the STP forecasts and the Persistence forecasts as shown in Figure 11 and in comparison with Figure 10.

Deleted: STP_{dist}
Formatted: Subscript
Formatted: English (US)
Deleted: STPdist
Deleted: Figure 9
Formatted: Subscript
Deleted: PRSdist
Formatted: Subscript
Formatted: Font:Not Italic
Formatted: Check spelling and grammar
Deleted: r
Deleted: results in
Deleted:
Deleted: all of the
Deleted: advantage
Deleted: methodology
Deleted: least improvement of the
Deleted: L-STP methodology relative to Persistence
Deleted: HF Radar
Deleted: capture similar
Deleted: periods
Deleted: repetition of the last velocity field persistently (during persistent periods)
Deleted: , shows
Deleted: the best
Deleted: , as the behavior of the flow will remain almost constant during the next few hours
Deleted: the persistent structure moves slightly from its original position
Deleted: clearly
Formatted: Font:Not Italic
Formatted: Check spelling and grammar
Deleted: Figure 10
Formatted: Check spelling and grammar
Deleted: Figure 9
Formatted: Font:Not Italic

We have compared the capabilities of the L-STP forecast against the forecast based on the persistency of currents. The L-STP method requires long training periods but performs better during non-persistent periods. Previous efforts to forecast surface currents from HFR data have shown similar results compared with the methodology presented in this paper. However, the advantage of the L-STP method is that it can be used in near real time, with short and non continuous datasets of around 2-3 years, provided that a Lagrangian catalog representative for the study area can be built.

Deleted: anytime

Deleted: , even if that data set contains temporal gaps

The HFR Progs MATLAB package (https://cencalarchive.org/~cocmpmb/COCMPwiki) has been used to generate total currents from radial files to fill the spatial gaps of the surface current field using the OMA method, and to generate Lagrangian trajectories. This methodology could be easily included in this package so the final users could get forecast currents, in the same time that they generate total currents.

5. *CONCLUSION*

A methodology to short term forecast of the surface currents in real-time has been proposed. This methodology provides accurate forecast of sea surface currents and its capability has been tested in terms of spatial and temporal distributions. The good functioning and confidence of this methodology has been demonstrated in the previous sections and also, its capability to be applied in real time. The methodology has been successfully applied to two distinct coastal regions to evaluate its capabilities in different hydrodynamic regimes, although further analysis using data from more areas is required to generalize the methodology.

Relationships between ε_{ANL} and ε_{STP}/ ε_{PRS} suggest that the ε_{ANL} can be considered as a reliable indicator of the method's performance. Taking in consideration all the analyses done in this work, we propose to use STP currents for trajectory or velocity field predictions from 12 hours foreward, if the ε_{ANL} value is lower than 80% of the cumulative ε_{ANL}. If ε_{ANL} is higher, or the forecast is just for the next 6 hours, the use of the persistence field is suggested. We also suggest that the ε_{ANL} value and forecast transition time need to be carefully evaluated for each study region. This, of course, infers that a minimum data set is required before the L-STP method can be applied.

Further analysis of analogue finding approaches is required to improve the observed results, especially during periods when currents are persistent. The use of longer dataset as a training period may improve this aspect. Then, the next step would be to test the methodology for additional periods and other regions, to analyze the possibility to find analogues for different sub-regions and to evaluate its functionality in an operational mode.

Deleted: se

Deleted: 2

Deleted: conditions

Deleted: . A

Deleted: , these initial results indicate that it works similarly in the 2 different analyzed study areas, suggesting that it can be generalized.

Deleted: ... [21]

Deleted: well-functioning

Deleted: (714 km^2 in the case of the BoB HFR system).

Deleted: last available hour, as persistent current

Deleted: began to

Deleted: ag

Deleted: help on this as well

The methods to find the minimum training period for each system should be analyzed deeper in future works. The minimum training period will be directly related to the variability of the local dynamics and those should be considered during the analysis.

Deleted: analysis

Deleted: , as the application of the STP forecast to the Red Sea HFR system should improve as the observational time period increases

Deleted: In case of an oil spill, the proposed methodology offers an accurate forecast of the surface currents for up to 48 hours in advance. But it is important to note that for the oil spill prediction, the influence of the wind and waves in combination with the surface currents also needs to be considered.

DATA AVAILABILITY

The Red Sea HF Radar data can be requested through:

- https://lthdatalib.kaust.edu.sa

Historical and NRT Bay of Biscay HF Radar data can be requested through:

- Euskoos portal: https://www.euskoos.eus/en/data/basque-ocean-meteorological-network/high-frequency-coastal-radars/
- Emodnet Physics - http://www.emodnetphysics.eu/Map/platinfo/piradar.aspx?platformid=10273
- CMEMS Instac - http://marine.copernicus.eu/services-portfolio/access-to-products/?option=com_csw&view=details&product_id=INSITU_GLO_UV_NRT_OBSERVATIONS_013_048

Formatted: Spanish

Field Code Changed

Formatted: Spanish

Formatted: Spanish

AUTHORS CONTRIBUTION

- Lohitzune Solabarrieta: She has worked on the set up of the methodology, data analysis, manuscript writing and final submission.
- Ismael Hernandez-Carrasco: He has worked on the set up of the methodology and the manuscript writing.
- Anna Rubio: She has worked on the set up of the methodology, data analysis, and manuscript writing.
- Alejandro Orfila: He has worked on the configuration of the methodology, data analysis and the manuscript writing.
- Michael Campbell: He has worked on the configuration of the methodology, especially in the pre-configuration that led us to rule out other data prediction methodologies. He has also contributed on the manuscript writing.
- Ganix Esnaola: He has worked on the configuration of the methodology, especially in the pre-configuration that moved us to the usage of analogues on this paper. He has also contributed on the manuscript writing.
- Julien Mader: He has contributed on the writing of the manuscript.
- Burton H. Jones: He has contributed on the writing of the manuscript

COMPETING INTERESTS

The authors declare that we have no conflict of interest

ACKNOWLEDGEMENTS

This work was funded by a Saudi Aramco-KAUST Center for Marine Environmental Observation (SAKMEO) Postdoc fellowship to Lohitzune Solabarrieta, and from the Integrated Ocean Processes (IOP) Group in KAUST. We acknowledge the support of the LIFE-LEMA project (LIFE15 ENV/ES/000252), the European Union's Horizon 2020 research and innovation program under grant agreement No. 654410 & 871153 (JERICO-NEXT and JERICO-S3 Projects), the Directorate of Emergency Attention and Meteorology of the Basque Government, the MINECO/FEDER Projects MUSA and MOCCA (CTM2015-66225-C2-2-P; 256RTI2018-093941-B-C31). and the Department of Environment, Regional Planning, Agriculture and Fisheries of the Basque Government (Marco Program). This work was partially performed while A. Orfila was a visiting scientist at the Earth, Environmental and Planetary Sciences Department at Brown University through a Ministerio de Ciencia, Innovación y Universidades fellowship (PRX18/00218). Ismael Hernandez-Carrasco acknowledges the Vicenç Mut contract funded by the Balearic Island Govern and the European Social Fund (ESF) Operational Programme.

The HF radar-processing toolbox HFR_Progs use to produce OMA was provided by D. Kaplan and M. Cook, Naval Postgraduate School, Monterey, CA, USA.

REFERENCES

Abascal, A. J., Castanedo, S., Medina, R., Losada, I. J., Álvarez-Fanjul, E.: Application of HF radar currents to oil spill modelling. Mar. Pollut. Bull. 58 (2), 238–248, 2009

Abascal A. J., Sanchez, J., Chiri, H., Ferrer, M. I., Cárdenas, M., Gallego, A., Castanedo, S., Medina, R., Alonso-Martirena, A., Berx, B., Turrell, W. R., Hughes, S. L.: Operational oil spill trajectory modelling using HF radar currents: A northwest European continental shelf case study. Marine Pollution Bulletin, Volume 119, Issue 1, Pages 336-350, ISSN 0025-326X, https://doi.org/10.1016/j.marpolbul.2017.04.010, 2017.

Abualnaja, Y., Papadopoulos, V. P., Josey, S. A., Hoteit, I., Kontoyiannis, H., and Raitsos, D. E.: Impacts of climate modes on air–sea heat exchange in the Red Sea, J. Clim., 28, 2665–2681, doi:10.1175/JCLI-D-14-00379.1, 2015.

Barrick, D. E.: Extraction of wave parameters from measured HF radar sea-echo Doppler spectra. Radio Sci., 12, 415–424, doi:10.1029/RS012i003p00415, 1977.

Barrick D.E., Fernandez, V., Ferrer, M.I., Whelan, C., and Breivik, Ø.: "A short-term predictive system for surface currents from a rapidly deployed coastal HF-Radar network," Ocean Dyn., vol. 62, no. 5, pp. 725–740, 2012.

Barth, A., Alvera-Azcárate, A., Beckers, JM., Staneva J., Stanev E.V., and Schulz-Stellenfleth J.: Correcting surface winds by assimilating high-frequency radar surface currents in the German Bight. Ocean Dynamics, 2011, vol 61: 599. https://doi.org/10.1007/s10236-010-0369-0, 2011.

Bellomo, L., Griffa, A., Cosoli, S., Falco, P., Gerin, R., Iermano, I., Kalampokis, A., Kokkini, Z., Lana, A., Magaldi, M.G., Mamoutos, I., Mantovani, C., Marmain, J., Potiris, E., Sayol, J.M., Barbin, Y., Berta, M., Borghini, M., Bussani, A., Corgnati, L., Dagneaux, Q., Gaggelli, J., Guterman, P., Mallarino, D., Mazzoldi, A., Molcard, A., Orfila, A., Poulain, P. M., Quentin, C., Tintoré, J., Uttieri, M., Vetrano, A, Zambianchi, E. and Zervakis, V.: Toward an integrated HF radar network in the Mediterranean Sea to improve search and rescue and oil spill response: the TOSCA project experience. Toward an integrated HF radar network in the Mediterranean Sea to improve search and rescue and oil spill response: the TOSCA project experience, Journal of Operational Oceanography, 8:2, 95-107, DOI: 10.1080/1755876X.2015.1087184, 2015.

Bower, A. S., and Farrar, J. T.: Air–sea interaction and horizontal circulation in the Red Sea. In N. M. A. Rasul & I. C. F. Stewart, (Eds.), The Red Sea, Springer Earth System Sciences (pp. 329–342). Berlin, Germany: Springer. https://doi.org/10.1007/978-3-662-45201-1_19, 2015.

Breivik, Ø, and Saetra, Ø.: Real time assimilation of HF radar currents into a coastal ocean model. Journal of Marine Systems, Volume 28, Issues 3–4, April 2001, Pages 161-182. https://doi.org/10.1016/S0924-7963(01)00002-1, 2001.

Chao, Y., Li Z., Farrara, K., McWilliams, J.C., Bellingham, J., Capet, X., Chavez, F., Choi, J., Davis, R., Doyle, J., Fratantoni, D. M., Li P., Marchesiello, P., Moline, M.A., Paduan, J., Ramp, S.: Development, implementation and evaluation of a data-assimilative ocean forecasting system off the central California coast. Deep Sea Research, Vol. 56, Issues 3-5, pp 100-126. https://doi.org/10.1016/j.dsr2.2008.08.011, 2009.

Crombie, D. D.: Dopler Spectrum of Sea Echo at 13.56-Mc/s', Nature 175, 681-682, 1955.

Emery, B. M., Washburn L., and Harlan, J. A.: Evaluating radial current measurements from CODAR high-frequency radars with moored current meters. J. Atmos. Oceanic Tech- nol., 21, 1259–1271, doi:10.1175/1520-0426(2004)021,1259: ERCMFC.2.0.CO;2, 2004.

Esnaola, G., Sáenz, J., Zorita, E., Fontán, A., Valencia, V., and Lazure, P.: Daily scale wintertime sea surface temperature and IPC-Navidad variability in the southern Bay of Biscay from 1981 to 2010, Ocean Sci., 9, 655–679, https://doi.org/10.5194/os-9-655-2013, 2013.

Fernández-Ferrero, A., Sáenz, J., Ibarra-Berastegi, G., Fernández, J.: Evaluation of statistical downscaling in short range precipitation forecast. Atmos. Res. 94, 448–461, 2009.

Fernández-Ferrero, A., Sáenz, J., Ibarra-Berastegi, G.: Comparison of the performance of different Analog-Based Bayesian probabilistic precipitation forecasts over Bilbao, Spain. Mon. Weather Rev. 38, 3107–3119, 2010.

Frolov, S., Paduan J., Cook M., and Bellingham J.: Improved statistical prediction of surface currents based on historic HF- radar observations. Ocean Dyn., 62, 1111–1122, doi:10.1007/ s10236-012-0553-5, 2012.

Hammond, T.M., Pattiaratchi ,C.B., Osborne, M.J., Nash, L.A., Collins, M.B.: Ocean surface current radar (OSCR) vector measurements on the inner continental shelf. Continental Shelf Research. Volume 7, Issue 4, Pages 411-431. https://doi.org/10.1016/0278-4343(87)90108-7, 1987.

Hernández-Carrasco, I., Solabarrieta, L., Rubio, A., Esnaola, G., Reyes, E., and Orfila, A.: Impact of HF radar current gap-filling methodologies on the Lagrangian assessment of coastal dynamics, Ocean Sci., 14, 827-847, https://doi.org/10.5194/os-14-827-2018, 2018.

Hernández-Carrasco, I., Orfila, A., Rossi, V., and Garçon, V.: Effect of small-scale transport processes on phytoplankton distribution in coastal seas, Scientific Reports, 8:8613, https://doi.org/10.1038/s41598-018-26857-9, 2018b.

Ibarra-Berastegi, G., Saenz, J., Ezcurra, A., Ezcurra, A., Elias, A., Diaz Argandona, J., Errasti, I.: Downscaling of surface moisture flux and precipitation in the Ebro Valley (Spain) using analogues and analogues followed by random

Formatted: English (US)

Formatted: English (US)

Formatted: English (US)

Formatted: English (US)

Formatted: English (US)

forests and multiple linear regression. Hydrol. Earth Syst. Sci. 15 (6), 1895–1907, 2011.

Jianping H., Yuhong Y., Shaowy W and Jifen C.: An analogue-dynamical long-range numerical weather prediction system incorporating historical evolution. Q. J. R. Meteorol. Soc., 119, pp.547-565, 1993.

Kaplan, D. M. and Lekien, F.: Spatial interpolation and filtering of surface current data based on open-boundary modal analysis, Journal of Geophysical Research: Oceans, 112, https://doi.org/10.1029/2006JC003984, c12007, 2007.

Kohut, J.T., Glenn, S.M.: Improving HF radar surface current measurements with measured antenna beam patterns. J. Atmos. Oceanic Technol. 20 (9), 1303–1316, 2003.

Lana, A., Marmain, J., Fernández, V., Tintoré, J., Orfila A.: Wind influence on surface current variability in the Ibiza Channel from HF Radar. Ocean Dynamics, 66: 483. https://doi.org/10.1007/s10236-016-0929-z, 2016

Langodan S., Cavaleri L., Vishwanadhapalli Y., Pomaro A., Bertotti L., Hoteit I.:. Climatology of the Red Sea - Part 1: the wind. Int. J. Climatol. 37: 4509–4517. DOI: 10.1002/joc.5103, 2017.

Liu Y., Weisberg, R.H., and Merz, C.R.: Assessment of CODAR SeaSonde and WERA HF Radars in Mapping Surface Currents on the West Florida Shelf. Journal of atmospheric and oceanic technology, Vol 31., pp 1363:1382, 2014.

Lorenz, E. N.: Atmospheric Predictability as Revealed by Naturally Ocurring Analogues. Journal of Atmospheric Sciences, Volume 29, pp 636-646, 1969.

Martin, M.L., Valero, F., Pascual, A., Sanz, J., and Frias, L.: Analysis of wind power productions by means of an analog model. Atmos. Res. 143, 238–249, 2014.

Oke, P. R., Allen, J. S., Miller, R. N., Egbert, G. D., and Kosro P. M.: Assimilation of surface velocity data into a primitive equation coastal ocean model, J. Geophys. Res., 107, 3122, doi:10.1029/2000JC000511, 2002.

Orfila A., Molcard, A., Sayol, J.M., Marmain, J., Bellomo, L., Quentin, C., and Barbin, Y.: Empirical Forecasting of HF-Radar Velocity Using Genetic Algorithms IEEE Transactions on Geoscience and Remote Sensing, Vol. 53, No. 5, 2015.

Ohlmann, C., White, P., Washburn, L., Emery, B., Terrill, E., Otero, M.: Interpretation of coastal HF radar–derived surface currents with high-resolution drifter data. J. Atmos. Oceanic Technol. 24 (4), 666–680, 2007.

Paduan, J.D., and Rosenfeld, L.K.: Remotely sensed surface currents in Monterey Bay from shore-based HF radar (coastal ocean dynamics application radar. J. Geophys. Res. 101 (C9), 20669–20686, 1996.

Paduan, J.D., and Shulman, I.: HF radar data assimilation in the Monterey Bay area. J. Geophys Res. 109:C07S09, 2004.

Paduan, J.D., Kim, K.C., Cook, M. S., and Chavez, F.P.: Calibration and Validation of Direction-Finding High-Frequency Radar Ocean Surface Current Observations. IEEE Journal of oceanic engineering, Vol. 31, No. 4, 2006.

Paduan, J.D., and Washburn, L.: High-Frequency Radar Observations of Ocean Surface Currents. Annual Rev. Marine. Sci. 2013.5:115-136, 2013.

Prince, K., X. and Goswami, B., N.: An Analog Method for Real-Time Forecasting of Summer Monsoon Subseasonal Variability. Monthly weather review, Vol 135, pp: 4149-4160. https://doi.org/10.1175/2007MWR1854.1, 2007.

Ren L., Miaro, J., Li Y., Luo, X., Li J. and Hartnett, M.: Estimation of Coastal Currents Using a Soft Computing Method: A Case Study in Galway Bay, Ireland. Mar. Sci. Eng., 7(5), 157; https://doi.org/10.3390/jmse7050157, 2019

Roarty, H., Cook, T., Hazard, L., George, D., Harlan, J., Cosoli, S., Wyatt, L., Alvarez Fanjul, E., Terrill, E., Otero, M., Largier, J., Glenn, S., Ebuchi, N., Whitehouse, B., Bartlett, K., Mader, J., Rubio, A., Corgnati, L., Mantovani, C., Griffa, A., Reyes, E., Lorente, P., Flores-Vidal, X., Saavedra-Matta, K.J., Rogowski, P., Prukpitikul, S., Lee, S.H., Lai, J.W., Guerin, C.A., Sanchez, J., Hansen, B. and Grilli, S.: The Global High Frequency Radar Network. Front. Mar. Sci. 6:164. doi: 10.3389/fmars.2019.00164, 2019 (in press).

Schmidt, R.: Multiple emitter location and signal parameter estimation. IEEE Trans. Antennas Propag., 34, 276–280, doi:10.1109/TAP.1986.1143830, 1986.

Schott F., Frisch, A.S., Leaman, K., Samuels, G., Popa Fotino, I.: High-Frequency Doppler Radar Measurementsof the Florida Current in Summer 1983. J. Geo. Research, Vol 90, No C5, pp 9006:9016, 1985.

Seubert, S., Fernández-Montes, S., Philipp, A., Hertig, E., Jacobeit, J., Vogt, G., Paxian, A., Paeth, H.: Mediterranean climate extremes in synoptic downscaling assessments. Theor. Appl. Climatol. 117 (1–2), 257–275, 2014.

Shao, Q. and Li, M.: An improved statistical analogue downscaling procedure for seasonal precipitation forecast . Stoch Environ Res Risk Assess 27, pp.: 819-830. https://doi.org/10.1007/s00477-012-0610-0, 2013.

Sofianos, S. S., and Johns, W. E.: An oceanic general circulation model (OGCM) investigation of the Red Sea circulation: 2. Three- dimensional circulation in the Red Sea. Journal of Geophysical Research, 108(C3), 3066. https://doi.org/10.1029/2001jc001185, 2003.

Solabarrieta, L., Rubio, A., Castanedo, S., Medina, R., Charria, G., Hernández, C.: Surface water circulation patterns in the southeastern Bay of Biscay: new evidences from HF radar data. Cont Shelf Res 74:60–76 doi:10.1016/j.csr.2013.11.022, 2014.

Solabarrieta, L., Rubio, A., Cárdenas, M., Castanedo, S., Esnaola, G., Méndez, F.J., Medina, R., and Ferrer, L.: Probabilistic relationships be- tween wind and surface water circulation patterns in the SE Bay of Biscay. Ocean Dyn., 65, 1289–1303, doi:10.1007/s10236-015-0871-5, 2015.

Solabarrieta, L., Frolov, S., Cook, M., Paduan, J., Rubio, A., González, M., Mader, J., and Charria, G.: Skill Assessment of HF Radar–Derived Products for Lagrangian Simulations in the Bay of Biscay. J. Atmos. Oceanic Technol., 33, 2585–2597, doi: 10.1175/JTECH-D-16-0045.1, 2016.

Stanev, E.V., Schulz-Stellenfleth, J., Staneva, J., Grayek, S., Seemann, J. and Petersen, W.: Coastal observing and forecasting system for the German Bight – estimas of hydrophysical states. Ocean Sci., 7, 569–583, 2011 doi:10.5194/os-7-569-2011, 2011.

Ullman, D.S., O'Donnell, J., Kohut, J., Fake, T., Allen, A.: Trajectory prediction using HF radar surface currents: Monte Carlo simulations of prediction uncertainties. J. Geophys. Res. 111 (C12005), 1–14, 2006.

Vilibić, I., Šepić, J., Mihanović, H., Kalinić, H., Cosoli, S., Janeković, I., Žagar, N., Jesenko, B., Tudor, M., Dadić, V. dnd Ivanković, D.: Self-organizing maps-based ocean currents forecasting system. Scientific Reports 6, 22924, 2016.

Yao, F., Hoteit, I., Pratt, L. J., Bower, A. S., Zhai, P., Kohl, A., and Gopalakrishnan, G.: Seasonal overturning circulation in the Red Sea: 1. Model validation and summer circulation, J. Geophys. Res. Oceans, 119, doi:10.1002/2013JC009004, 2014.

Yao, F., Hoteit, I., Pratt, L. J., Bower, A. S., Kohl, A., Gopalakrishnan, G., and Rivas, D.: Seasonal overturning circulation in the Red Sea: 2. Winter circulation, J. Geophys. Res. Oceans, 119, 2263–2289, doi:10.1002/2013JC009331, 2014.

Zarokanellos, N. D., Kürten, B., Churchill, J. H., Roder, C., Voolstra, C. R., Abualnaja, Y., and Jones, B. H.: Physical mechanisms routing nutrients in the central Red Sea. Journal of Geophysical Research: Oceans, 122. https://doi.org/10.1002/2017JC013017, 2017a.

Zarokanellos, N. D., Papadopoulos, V. P., Sofianos, S. S., and Jones, B. H.: Physical and biological characteristics of the winter-summer transition in the Central Red Sea. Journal of Geophysical Research: Oceans, 122, 6355–6370. https://doi.org/10.1002/2017JC012882, 2017b.

Zhan, P., Subramanian, A. C., Yao, F., and Hoteit, I.: Eddies in the Red Sea: A statistical and dynamical study, J. Geophys. Res. Oceans, 119, 3909–3925, doi:10.1002/2013JC009563, 2014.

Zelenke B. C.: An Empirical Statistical Model Relating Winds and Ocean Surface Currents. Master of Science in Oceanography - Thesis, Oregon State University, 2005.

Zorita E, and von Storch H.: The analog method as a simple statistical downscaling technique: comparison with more complicated methods. J Climate 12:2474–2489, 1999.

TABLES

Table 1: Characteristics of the previously developed STP works based on HFR data.

Authors	Approach	Needs continuous training period	Comple-mentary data required?	Region of application	Reliable forecast period
Zelenke 2005	EOF + bilinear regression model	Yes	Wind	Oregon coast	48 hours
Frolov et al. 2012	EOF + linear auto regression model	Yes	Wind and tides (optional)	Monterey Bay, California	48 hours
Barrick et al., 2012	Constant linear trend model applied to OMA modes	Yes	Wind	Finnmark, Norway	12 hours
Orfila et al. 2015	EOF+Genetic Algorithm	Yes	No	Toulon, France	48 hours
Solabarrieta et al. 2016	Frolov et al., 2012	Yes	No	Bay of Biscay	48 hours
Vilibić et al., 2016	SOM+neural network +winds	Yes	Wind	Northern Adriatic Sea	72 h
Ren et al., 2019	Random Forest (RF) classification algorithm	No	Tide and Wind	Galway Bay, Ireland	59 h
This paper: L-STP	Analogue finding	No	No	Bay of Biscay and the Central Red Sea	48 h

Table 2: Correlation coefficient values between winner ε_{ANL} and δ_{STP} and between ε_{ANL} and δ_PRS, after 6, 12, 24, 36 and 48 hours of simulation.

	6 hours	**12 hours**	**24 hours**	**36 hours**	**48 hours**
R^2 ε_{ANL} – δ_{STP}	0.19	0.37	0.55	0.56	0.54
R^2 ε_{ANL} – δ_{PRS}	0.07	0.11	0.03	0.01	0.04
ε_{ANL} [km2], for the inflection point between δ_{STP} and δ_{PRS}	-	714	774	857	1027
% of ε_{ANL} (accumulative) for the previous line	-	81	84	87	95

Deleted: *STP_{dist}*
Formatted: Subscript
Deleted: *PRS_{dist}*
Deleted: **STP_{dist}**
Formatted: Subscript
Deleted: **PRS_{dist}**
Formatted: Subscript
Deleted: STP_{dist}
Formatted: Subscript
Deleted: PRS_{dist}
Formatted: Subscript

FIGURES

Figure 1*: (Left) HFR system of the BoB. (Right) HFR system of the central Red Sea. Blue dots represent the data points and the black cross are the HFR antenna positions*

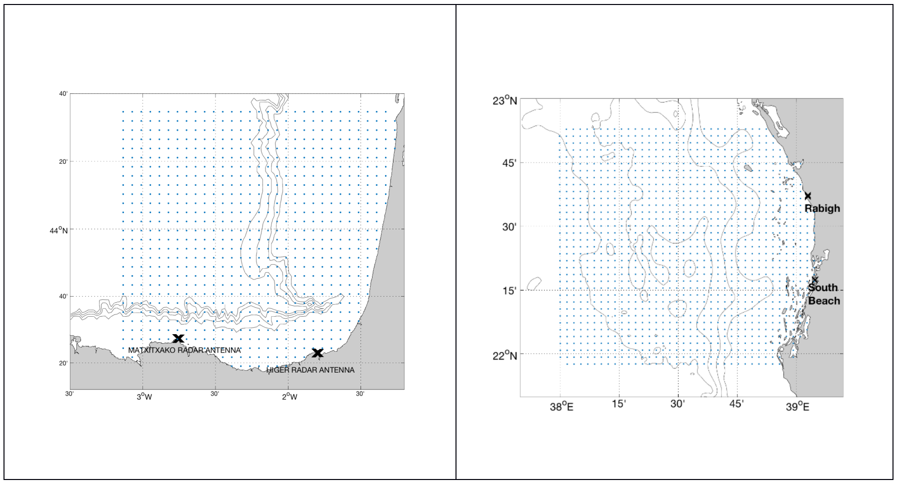

Figure 2: (1) 15-Apr-2015 00:00 example of the developed methodology applied to the BoB HFR system. (a) The past 48 hours of target field of test period (b) The analogue having the lowest error, (c) The truth trajectories for the forecast period (d) the STP trajectories. The initial positions of the particle trajectories are indicated by the blue dots, and the red dots indicate the position after 48 hours.

Deleted: ... [22]

Formatted: Font:14 pt

Deleted: 3

Deleted: *realized*

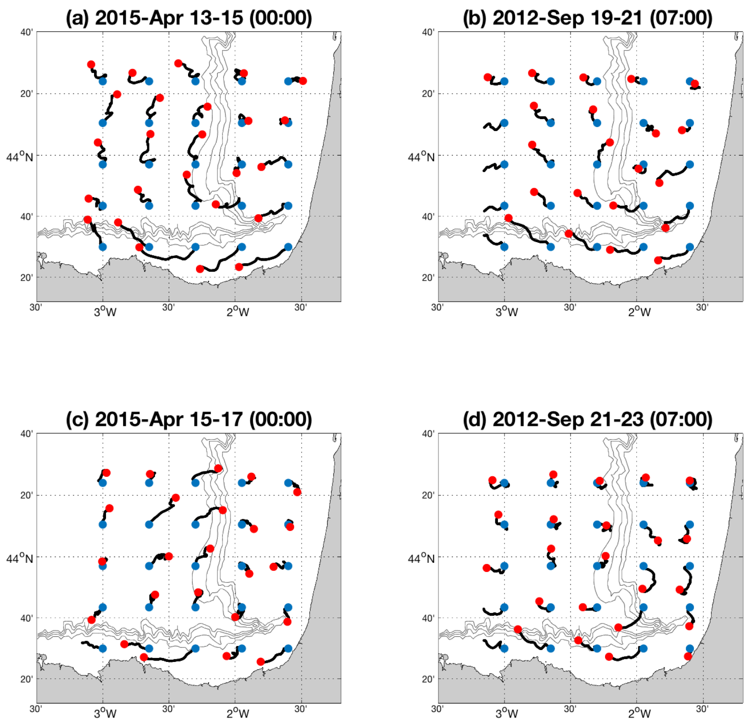

Figure 3: Example for the test period: 15-Apr-2015 00:00; errors for the whole Lagrangian catalogue fields of the BoB HFR System, restricted to the δ_cg = 10 km condition. The red dot indicates the occurrence date and the error of the winner analogue (19-Sep-2012 07:00).

Deleted: 4

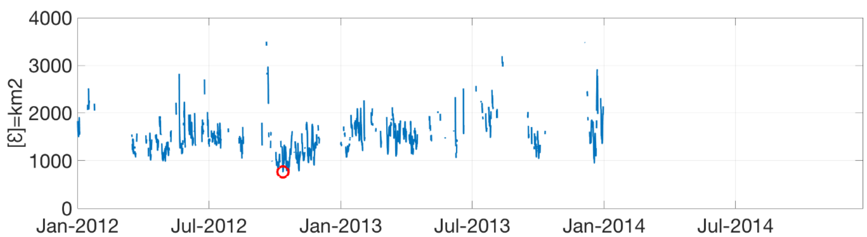

Formatted: Font:14 pt

Figure 4***: Scheme of the analogue selection and L-STP forecast assessment process.***

Formatted: Font:14 pt, Italic

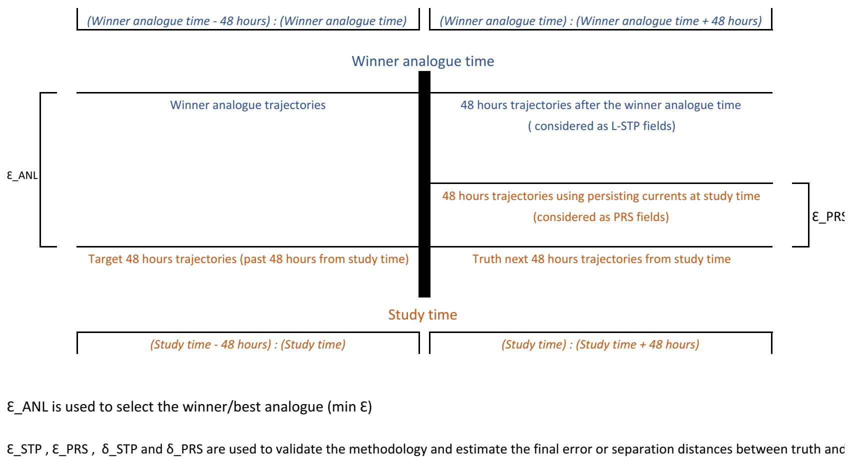

Figure 5: errors of the hourly winner analogue for 2015 (ε_{ANL}), together with the ε_{STP} and ε_{PRS}. The black dots over the timeline shows the times when ε_{STP} is higher than ε_{PRS}

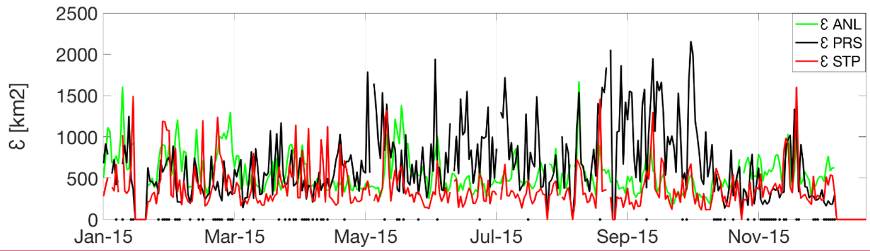

Deleted: 4

Deleted: *the STP error*

Deleted:

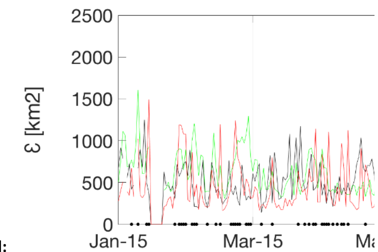

Formatted: Font:14 pt

Figure 6: X axis shows the ε_{ANL}, ordered from minimum to maximum, for the winner analogue for the test year 2015. Left Y axis indicates ε_{STP} (red) and ε_{PRS} (blue) for the corresponding ε_{ANL}. Right Y axis indicates the % of the accumulative comparison times as shown by the black solid line. Dashed vertical line indicates the crossing point between ε_{STP} and ε_{PRS} (ε_{ANL}=853Km2).

Deleted: 5

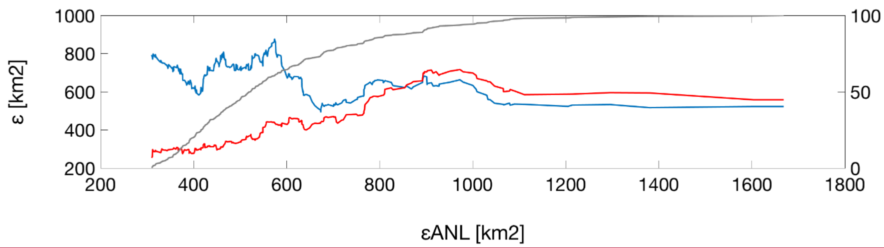

Deleted:

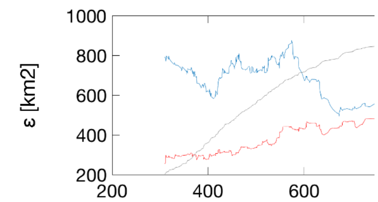

Formatted: Font:14 pt

Figure 7: Left Y axis indicates δ_{STP} (red) and δ_{PRS} (blue) for the corresponding ε_{ANL}, after 6, 12, 24, 36 and 48 hours. Right Y axis is the cumulative % of timesteps in the computation of the mean errors, as indicated by the black line in the plots. X axis is the ε_{ANL}, ordered from minimum to maximum, for the winner analogue for the test year 2015.

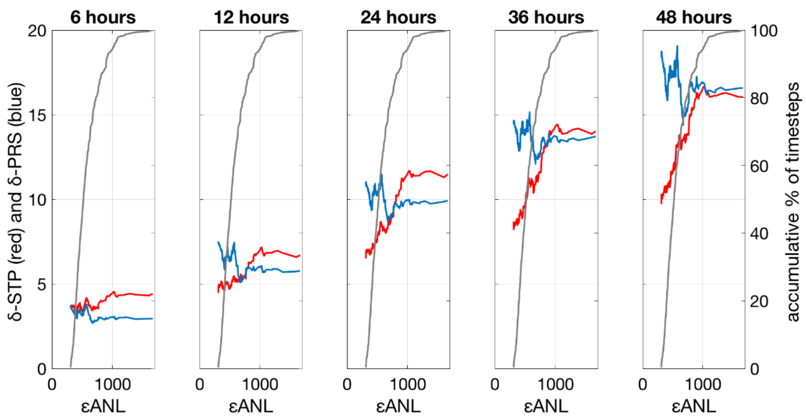

Deleted: 6

Deleted: STP_{dist}

Deleted: PRS_{dist}

Formatted: Subscript

Formatted: Subscript

Deleted:

Deleted:

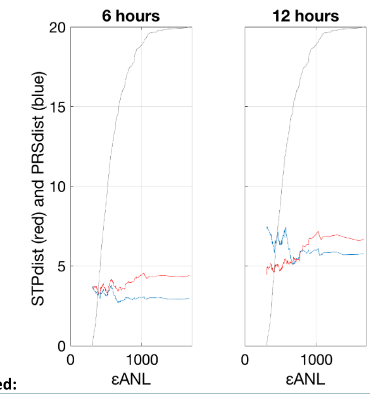

Formatted: Font:14 pt

Figure 8: Time evolution of the mean separation δ_{STP} and δ_{PRS} [km] between truth and forecast trajectories using truth and STP/PRS currents and the mean drift, with BoB system data, for 2015.

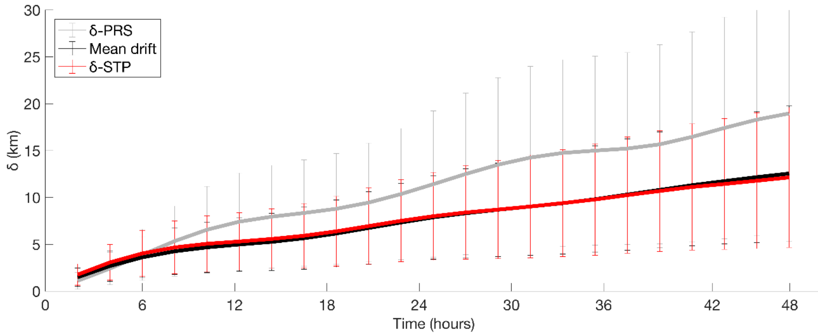

Deleted: 7
Deleted: *distances*
Deleted: *realized*
Deleted: *realized*
Deleted: ... [23]
Formatted: Font:Italic
Formatted: Font:Italic

Figure 9: Time evolution of the mean separation distances δ_{STP} and δ_{PRS} [km] between real and forecast trajectories using truth and STP/PRS currents and the mean drift, with the Red Sea HFR system data, for July 2017 to October 2018.

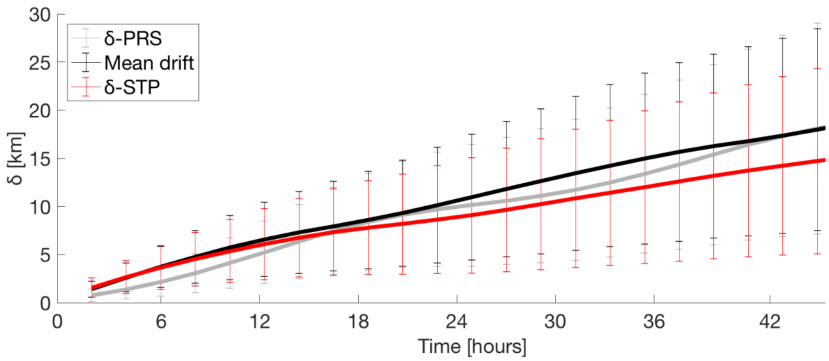

Deleted: 8

Deleted: (UP)

Formatted: Subscript

Deleted: *realized*

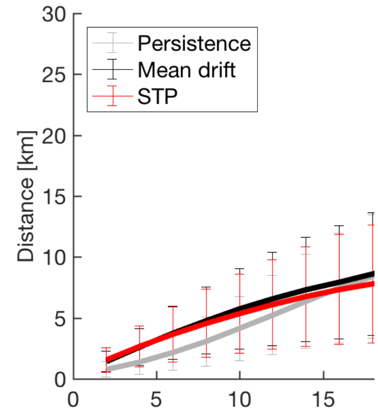

Deleted:

Formatted: Font:Italic

Formatted: Left

Formatted: Font:Italic

Figure 10: Spatial distribution of separation distances [km] between trajectories using L-STP and persistent currents at 6, 12, 24 and 48 hours, for the BoB HFR System.

Deleted: 9

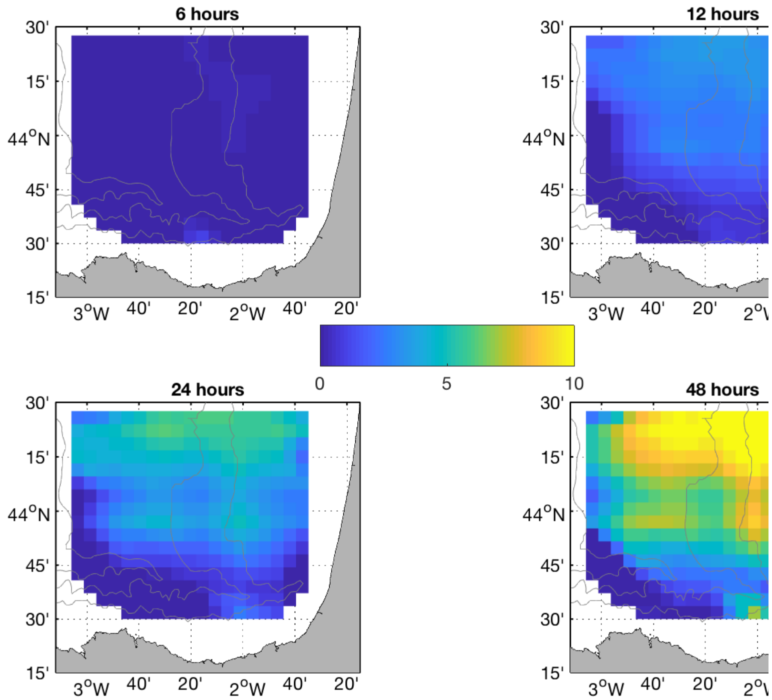

Deleted:

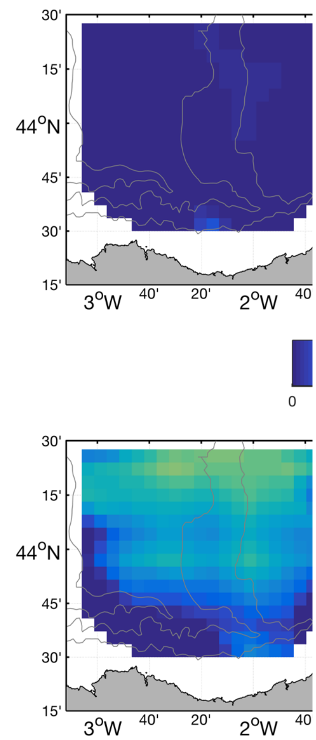

Formatted: Font:Italic

Figure 11: Spatial distribution of separation distances [km] between trajectories using L-STP and persistent currents at 6, 12, 24 and 48 hours, for the Red Sea HFR system.

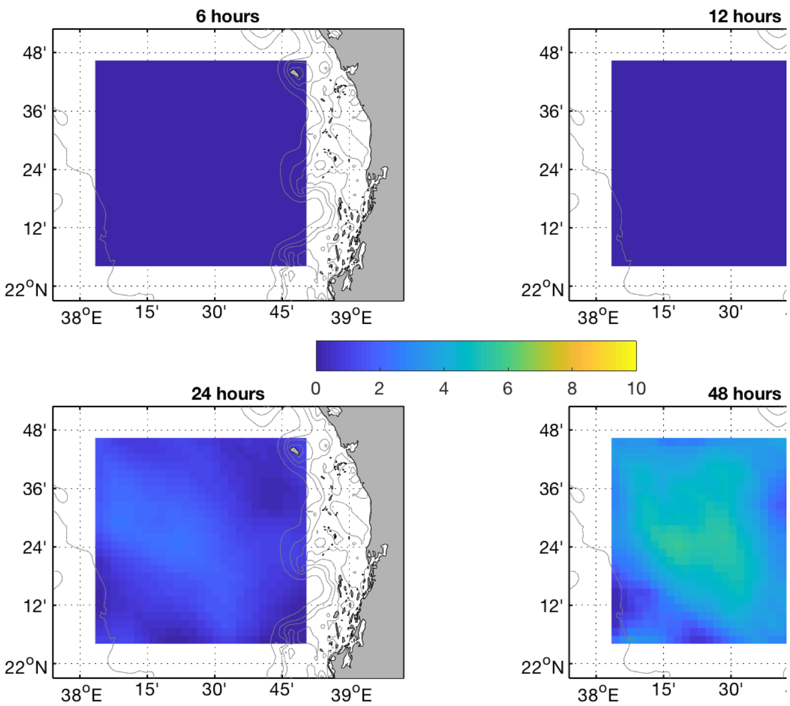

Deleted: 10

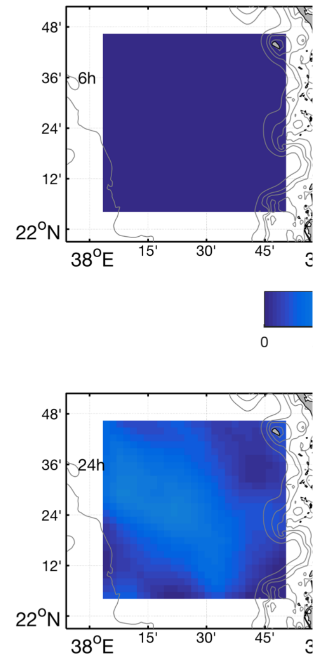

Deleted:

Formatted: Font:Italic

Formatted: Font:Italic